pump on/off cycles. General corrosion was observed in the threaded region for nearly all couplings, including those with no evidence of cracking. The couplings containing cracks exhibited pitting at the thread roots, and it appeared that SCC cracks emanated from the pits. Chemical analysis via EDS of IGSCC fracture surfaces exhibited detectable amounts of chlorine, which is indicative of chlorides, thereby providing evidence that this species contributed to the SCC. Other corrosive species that could contribute to SCC in the couplings may be present in the service water basin. To assess the aqueous environment experienced by the couplings, it is recommended that hydrogen sulfide and chloride concentration samples be taken at the packing leak-off drain line to determine if there any local differences in corrosive species concentration.

Finite element analysis (FEA) was used to model tensile stresses in couplings, which must be present for SCC to occur, along with a susceptible material and corrosive environment. The calculated peak tensile stresses at the thread root were estimated to be around 70 ksi, which is judged to be sufficient to enable SCC. However, the presence of pits may have increased the stress intensity such that SCC could occur at lower stress.

It was noted that Neolube was generously applied to couplings in pump P-7A, which did not exhibit cracks. Cracked couplings in pump P-7B had some Neolube, while failed and cracked couplings in pump P-7C had no noticeable amount of Neolube in the as-received condition. It is not clear if Neolube played a significant role in limiting pit formation and SCC in couplings. However, well-coated couplings in pump P-7A did not exhibit pits or cracks at the thread root even though it had been in service the longest and had the greatest run time upon extraction.

Metallurgical analysis of fractured and cracked couplings revealed SCC to be an issue for Type 416 SS couplings in the service environment. The wet and dry cycles experienced by couplings Nos. 5, 6, and 7 likely created elevated chloride levels that lead to pitting corrosion and SCC. As evidence, five out of nine couplings in the wet and dry region were found to contain SCC cracks. No cracks were found on tested couplings that were continuously submerged. Because Type 416 SS martensitic stainless steel is particularly susceptible to corrosion and SCC in halide environments and heat treatment to achieve the desired balance between hardness and toughness is difficult, this class of alloy is not an optimal choice for the service water pump couplings. It is recommended that a different material with superior corrosion resistance to SCC while maintaining designed strength requirements is selected.

6.0 REFERENCES

1. Entergy Palisades Root Cause Evaluation for CR-PLP-2009-04519, "Service Water Pump P-7C Failure to Provide Discharge Pressure" 3/4/2010, Rev. 1
2. Entergy Palisades Root Cause Evaluation Report for CR-PLP-2011-03902, "Service Water Pump 7-C Line Shaft Coupling Failure"
3. Entergy Palisades Drawing
   a. Entergy Drawing No.M-213, Rev. 93 "Piping and Instrumentation Diagram Service Water, Screen Structure and Chlorinator"
   b. Entergy Drawing No. VEN-M-11-Sht 45, Rev. 2 "Service Water Pumps Modified Line Shaft Components For Pumps P-7A, P-7B and P-7C"
   c. Entergy Drawing No. VEN-M-11-Sht 0055,
4. Entergy Engineering Change (EC)-50000121762
5. LPI Procedure F11358-P-001, "Procedure for Metallurgical Examination of SW Pump P-7C Coupling Components", Rev. 1
6. PLP Response to NRC Special Investigation Team RFI # 43 "Operating Service History Since Last Coupling Failure"
7. ASTM A582/A582M, "Standard Specification for Free-Machining Stainless Steel Bars", 2005.
8. ASTM E 18-07, "Standard Test Method for Rockwell Hardness of Metallic Materials"
9. ASTM E8/E8M-09, "Standard Test Methods for Tension Testing of Metallic Materials"
10. ASTM E23-07ae1 "Standard Test Methods for Notched Bar Impact Testing of Metallic Materials"
11. ASTM E3-11, "Standard Guide for Preparation of Metallographic Specimens"
12. ASTM E407-99, "Standard Practice for Microetching Metals and Alloys"
13. ANSYS Mechanical Software, ANSYS Inc., Southpoint, Canonsburg, PA 15317
14. OBERG E, et al. "Machinery's Handbook" 25th Ed. Industrial Press
15. HydroAire Calculation NQ5940, "Maximum combined shear stress calculation for threaded coupling", Rev. 3
16. LPI Procedure 4.1, "Software Control", Rev. 2
17. ANSYS Inc., LPI Report No. V&V-ANSYS-11, "Verification and Validation of ANSYS", Rev. 3
18. Shigley's, "Mechanical Engineering Design" McGraw Hill
19. Structural Integrity Report 1100112.401, "Additional Review of Palisades Service Water Pump Couplings", Rev. 0 March 2011.
20. HydroAire Inc. Drawing No. 1047237 "Line Shaft Coupling Johnstone 25 NMC 2 STG" Sht. 1/1, Rev. 1
21. Flowserve Materials Newsletter Volume 3, Number 4 "Embrittlement of Martensitic Stainless Steels", September 2004.

22. M.O. Speidel "Corrosion Fatigue in Fe-Ni-Cr Alloys", NACE-5 Stress Corrosion Cracking and Hydrogen Embrittlement of Iron Base Alloys, National Association of Corrosion Engineers, Houston, 1977, p. 1071 to 1094.
23. ASM Handbook, Volume 13A: Corrosion: Fundamentals, Testing, and Protection, "Stress-Corrosion Cracking", R.H. Jones, Battelle Pacific Northwest National Laborator, 2003 ASM International
24. ASM Handbook, Volume 11: Failure Analysis and Prevention, "Stress-Corrosion Cracking", Revised by W.R. Warke, 2002 ASM International
25. ASM Heat Treater's Guide: Practices and Procedures for Irons and Steels, Datasheet for 416, 416Se, 2nd Edition, ASM International 1995
26. ASM Metals handbook, Heat Treating, Cleaning and Finishing, 8th Edition Vol. 2
27. NRC Information Notice 2007-05: "Vertical Deep Draft Pump Shaft and Coupling Failures", February 9, 2007.
28. ASM Handbook, Volume 13A "Evaluating Stress-Corrosion Cracking", S.D. Cramer, B.S. Covino, Jr, Revised by Bopinder Phull
29. ASM Metals Handbook, "Corrosion" 9th Edition, Vol. 13, 1987, pp. 1129-1133
30. Palisades Nuclear Plant Work Instruction WI-SWS-M-03, "Service Water Pump P-7A Removal, Inspection, and Reinstallation", Rev. 4
31. Palisades Nuclear Plant Work Instruction WI-SWS-M-04, "Service Water Pumps P-7B and P-7C Removal, Inspection, and Reinstallation", Rev. 4
32. Pilkey, Walter "Peterson's Stress Concentration Factors", 2nd Edition,. © 1997 John Wiley & Sons
33. R.W. Hertzberg, "Deformation and Fracture Mechanics of Engineering Materials", 2nd Edition John Wiley & Sons.
34. Atlas Specialty Metals Tech Note No. 7, "Galvanic Corrosion", May 2006
35. Journal of Composite Materials Vol. 24, "Corrosion Between a Graphite/Polymer Composite and Metals" January 1990.
36. R.E. Avery, et al., "Stainless Steel for Potable Water Treatment Plants (PWTP) – Guidelines"

Lucius Pitkin, Inc. *Consulting Engineers*

Advanced Analysis
Fitness-For-Service
Failure & Materials Evaluation
Nondestructive Engineering

Est. 1885

September 28, 2011
LPI Ref. F11358-LR-001, Rev. 0

Mr. Alan Blind
Entergy Nuclear Operations, Inc.
Palisades Nuclear Plant
27780 Blue Star Memorial Highway
Covert, MI 49043

SUBJECT: Past Operability Assessment of Service Water Pumps P-7A and P-7B associated with As-found Evaluation of Pump Shaft Couplings – Palisades Nuclear Plant

LPI Project No. F11358
Entergy Contract No. 10325528

Dear Mr. Blind:

Lucius Pitkin, Inc. (**LPI**) is presently supporting Entergy Palisades Nuclear Plant (PLP) with an evaluation and assessment of Service Water System (SWS) pump couplings, following the failure of in-line pump shaft coupling No. 7, for Pump P-7C, as described in condition report CR-PLP-2011-03902 [2][1].

Palisades has requested a past operability assessment of service water pumps P-7A and P-7B, relative to the ability of the pump's shaft couplings to perform their function for a mission time of 30 days. At this time, LPI has examined couplings No. 4, 5, 6 and 7 removed from Pumps P-7A and P-7B, with respect to the failure assessment described within LPI Report F11358-R-001 [3] associated with the failure of pump P-7C coupling No. 6.

1.0 BACKGROUND

Failure of two pump couplings, No. 7 coupling in 2009 (referred to herein as 09-P7C-7F)[2] and No. 6 coupling in 2011 (11-P7C-6F), occurred on the P-7C pump, as described in [1 and 2]. The couplings were fabricated of ASTM A582 Type 416

[1] Numbers in [xx], i.e "4", refer to References listed in Section 5.0.
[2] Coupling naming convention used herein and in [3] refers to year of failure or examination-pump identity-coupling identifier. The F or K term is added if the identified coupling failed or cracked, respectively. Thus the 2009 failure of pump P-7C coupling number 7 is identified as 09-P7C-7F.

stainless steel (SS) material. A failure evaluation of these couplings was performed as described in [3], which identified the failure mode as intergranular stress corrosion cracking (IGSCC), resulting from a susceptible material (a martensitic steel found to have relatively low fracture toughness) operating in a corrosive environment and subjected to a threshold tensile stress. The report [3] also identified a crack approximately one-quarter through the wall in another coupling from the P-7C pump: coupling No. 7 (11-P7C-7K) that exhibited similar stress corrosion cracking (SCC) characteristics.

Each SW pump features eight (8) couplings, numbered 1 through 8. The present assessment has been focused on coupling Nos. 5, 6, and 7 for all service water pumps, since they are subjected to wet and dry cycles. Couplings 6 and 7 are subjected to wet and dry cycles dependent only upon pump usage state (i.e. on or off). Coupling 5 at approximately elevation 579' is dependent upon pump usage and water level (see Figure 1-1). Depending upon the time of year, water level in the service water basin (i.e. Lake Michigan level) ranges from elevation 576' to 580'. It is postulated in LPI report F11358-R-001 [3] that the wet/dry cycle enables the chlorides in the service water to concentrate at the thread roots of the coupling when the water drains from the coupling. This postulate is supported by fluorescent magnetic inspection testing (MT) of coupling 4 of each pump resulting in no indications. Unlike couplings 5, 6 and 7, coupling 4 is continuously submerged and does not typically experience wet/dry cycles.

Chlorides are present in the raw service water (water from Lake Michigan) in concentrations of approximately 9.7 ppm. The service water system is chlorinated on a daily basis to control algae and other microbes. After chlorination, the chloride levels increase to approximately 10 ppm. Thus, chlorination has little impact on the chloride levels in the service water. Chlorides in high humidity and oxygen rich environment are known to be corrosive agents resulting in IGSCC of martensitic stainless steels such as 416 SS.

2.0 EXAMINATION/TEST RESULTS

2.1 Pump P-7A Couplings

Pump P-7A coupling numbers 4, 5, 6 and 7 (coupling identifiers: 11-P7A-4, 11-P7A-5, 11-P7A-6, and 11-P7A-7, respectively) were submitted to LPI for examination on August 30, 2011. A photograph of the as-received coupling 11-P7A-7 is provided in Figure 2-1. Couplings 4 through 7 were visually examined and inspected by fluorescent magnetic particle inspection testing (MT). Couplings 5 through 7 were hardness tested, tensile tested, Charpy V-Notch (CVN) impacted tested and analyzed for material composition using methods as described in [3] for the P-7C pump couplings.

The results of the visual examination and MT inspection are shown in Figures 2-2 and 2-3, respectively. The threads of the P-7A couplings were found to be coated with lubricant, which has previously been identified by PLP maintenance as Neolube [4]. Following cleaning, the threads of couplings 4 through 7 were MT inspected and did not exhibit indications of linear flaws.

The couplings were tested with results summarized for: CVN impact energy in Table 2-1; Tensile Strength in Table 2-2; Material Composition in Table 2-3; Surface Hardness in Table 2-4, and Through Thickness Hardness in Table 2-5.

2.2 Pump P-7B Couplings

Pump P-7B coupling numbers 4, 5, 6 and 7 (coupling identifiers: 11-P7B-4, 11-P7B-5, 11-P7B-6, and 11-P7B-7, respectively) were submitted to LPI for examination on September 2, 2011. A photograph of the as-received couplings 11-P7B-4 through 11-P7B-7 is shown in Figure 2-4. Couplings 11-P7B-4 though 11-P7B-7 were split longitudinally for fluorescent magnetic particle inspection (MT). The as-split coupling 11-P7B-4 appeared to have been cleaned and exhibit a dye liquid penetrate residue on the threads (see Figure 2-5). The presence of the liquid penetrate on the thread surface is consistent with efforts by Palisades to examine this coupling for possible re-use due to procurement issues with the replacement couplings fabricated from 17-4PH material. As-split couplings 11-P7B-5 through 11-P7B-7 are shown in Figure 2-6 through Figure 2-8. Neolube is present on the threaded surfaces of coupling 11-P7B-5 to 11-P7B-7. However, an apparent band of corrosion product was observed at the center two-to-three threads of couplings 11-P7B-6 and 11-P7B-7. Coupling 11-P7B-5 also exhibited some corrosion at the center threads but not to the extent of couplings 11-P7B-6 and 11-P7B-7 (see Figure 2-6).

Following cleaning, couplings 11-P7B-4 through 11-P7B-7 were MT inspected. MT of couplings 11-P7B-4 through 11-P7B-7, revealed indications at the center (near location of corrosion products) of couplings 11-P7B-5, 11-P7B-6 and 11-P7B-7. An indication was also found at the motor end of coupling 11-P7B-5. No indication was found on coupling 11-P7B-4. Metallographic examination of the MT indications on 11-P7B-5K through 11-P7B-7K revealed a network of branched cracks initiating from pits at the thread roots (see Figure 2-9, Figure 2-10 and Figure 2-11). The branching network of cracks is indicative of SCC. A summary of the as-found cracks on the P-7B couplings follows:

Coupling	Crack Location	Crack Depth (in)	Crack Length (in)
B5	Center	0.065	1.25
	Motor End	0.02	0.25
B6	Center	0.132	0.5
B7	Center	0.043	0.5

Couplings 11-P7B-5K though 11-P7B-7K were tested with results summarized for: CVN impact energy in Table 2-1; Tensile Strength in Table 2-2; Material Composition in Table 2-3; Surface Hardness in Table 2-4, and Through Thickness Hardness in Table 2-5.

3.0 EVALUATION

3.1 Pump Run Time

The matrix below summarizes the SWS pump coupling service history at time of extraction.

SWS Pump Coupling Life						
Pump	Date Installed	Date Extracted	Installed Time (hrs)	Run Time (hrs)	Start/Stops	Notes
P-7A	4/4/09	8/28/11	21,024	16,259	148	1
P-7B	5/12/10	9/1/11	11,391	9,073	70	2
P-7C	6/12/09	9/29/09	2,616	2,414	13	3
P-7C	10/1/09	8/8/11	16,224	14,115	95	4

Notes:

1) Run hours and stops and starts based on total presented in Palisades response to NRC RFI 43 [5] plus average monthly hours from 4/10 to 9/10 times 6 months.
2) Information provided in Figure 3-0.
3) Information provided in Figure 3-1.
4) Run hours and stops and starts based on total presented in Palisades response to NRC RFI 43 [5].

3.2 Visual Inspection

3.2.1 Coupling P-7A

Visual inspection of the P-7A pump couplings 11-P7A-4 through -7 identified the threads to be well coated with lubricant (as-received). This was in contrast to observations of the P-7C couplings in the as-received condition, where lubricant was not observed to be as well coated on the threads. A comparison of this is shown in Figure 3-2. The coating of lubricant on the P-7A couplings could enhance pitting resistance.

3.2.2 Coupling P-7B

Visual inspection of the P-7B pump couplings 11-P7B-4, 11-P7B-5K, 11-P7B-6K, and 11-P7B-7K show the couplings to be generally well coated with Neolube. However, the amounts were generally less than that observed on couplings 11-P7A-4 through 11-P7A-7.

Stereomicroscopy of the coupling thread roots indicated that couplings exhibiting cracks tend to contain pitting, whereas couplings without indications contained less or no pitting. That is, pits or cracks were not observed in couplings 11-P7A-4 through 11-P7A-7 and 11-P7B-4, whereas couplings 11-P7B-5 through 11-P7B-7 contained pits and cracks. Figure 3-3 presents a representative comparison of a coupling without pits (and with no indications) and couplings that exhibit pits and contain cracks.

Based on the amount of Neolube on the coupling of P-7A and the absence of observed pits or cracks at the thread roots, it is postulated that the Neolube provided a protective coating that enhanced the corrosion resistance of the P-7A couplings.

3.3 Metallurgical / Environmental

Chemical composition and tensile testing of all tested P-7A and P-7B couplings indicates that the couplings are within specification for ASTM A582 Type 416 martensitic stainless steel. CVN impact energy test results ranged from 3 ft-lb to 16 ft-lb for tests at 32°F. ASTM A582 does not specify an impact energy requirement. CVN impact energy, tensile properties and chemical composition did not directly correlate with cracked and un-cracked couplings. Coupling 11-P7A-6 had low impact energy (3 ft-lb at 32°F) and did not exhibit cracks, whereas coupling 11-P7B-7 had higher impact energy (11 to 14 ft-lb at 32°F) and contained cracks.

Based on composition and CVN impact energy test results, all examined couplings are considered within the range of susceptibility to SCC since the environment to which the couplings are subjected is postulated to be the same. This postulation is based on the pumps extracting service water from the same basin. However, the observation of SCC in examined couplings from pumps P-7C and P-7B, but not examined couplings from P-7A, could be attributed to the Neolube and/or the third criterion for SCC, tensile stress. Also, based on the run time data provided in Section 3.1, it can be seen that the P-7A pump and couplings have been in service longer, experienced more run time and starts and stops than the other two service water pumps but yet the examined P-7A couplings are free of cracks. Since the environment[3] and material susceptibility is essentially the same for all service water pumps, the other contributors to SCC, applied tensile stress is investigated. Tensile stress in couplings of P-7C, P-7B and P-7A could differ due to thread form fit between the shaft and couplings.

3.4 Tensile Stress

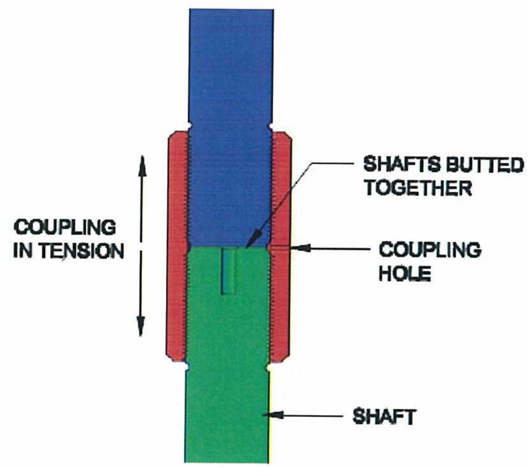

The coupling and shafts are assembled to ensure equal threading of the two shafts within a coupling by the use of an alignment aid inserted in the 1/8" hole on the side of the coupling. Once the shafts touch the alignment aid it is removed and motor torque is relied upon to tighten up the shaft-coupling assembly. With application of motor torque the two shafts will tighten and bear against each other within the coupling (see figure to right) which will induce compression on the shaft. The shaft compression is reacted as tension across the coupling. Also when the shafts butt up against each other within the coupling, a circumferential gap between the shaft and coupling is created due to the end geometry of the two shafts. The gap in conjunction with the alignment hole would enable deposits to collect at the exposed thread roots of the shaft intersecting plane.

To estimate the tensile stress across the coupling, a finite element analysis (FEA) model of a coupling was developed. A half FEA model of an intact coupling was developed using ANSYS and consists of the steel body, alignment hole and threads. The model was constructed of the eight-node brick element, SOLID45 (see Figure 3-4). The symmetric boundary condition, $U_z=0$ and $U_\theta=0$, is applied on the inner surface as shown in Figure 3-5. ASTM A582 Type 416 stainless steel material property for the coupling FEA model is as follows:

Young's modulus: 29.2×10^6 psi
Poisson's ratio: 0.3

[3] Although as outlined in Section 3.2.1, the presence of liberal amounts of Neolube on the P7A couplings could play a significant role in protecting those threads from the corrosive environment.

Coupling threads are 2-3/16, 8 TPI which is not a common thread form. Specific thread properties are not available in the Machinery's Handbook [11]. Therefore, internal thread properties of the coupling is taken to be the average internal diameter of 2-1/4, 8 TPI and 2-1/16, 8 TPI in the Machinery's Handbook [11].

Loading on the coupling model consists of the weight of components below the coupling, hydraulic thrust and motor torque. These loads are extracted from HydroAire calculation NQ5940 [12]. Motor torque is transmitted across the coupling by bearing of the shaft ends against each other within the coupling.

The resulting stress distribution across the wall of the coupling at the middle thread root of the coupling, as determined from the FEA model is presented in Figure 3-6. The Figure 3-6 stress distribution is based on reacting the applied shaft end compression load from the applied motor torque across three threads[4] per shaft end. Considering the two shafts meeting approximately in the center of the coupling, the three threads below the centerline react the lower shaft compression loading, the three threads above the centerline react the compression loading in the upper shaft. However, tolerances in machining of the threads could translate into different load and stress distribution across the threads. If the load is distributed to fewer or greater number of threads than the three assumed, then the tensile stress at the thread root could range according to the load distribution to the threads.

For example, if the shaft bearing loads were distributed across six threads instead of three, the maximum tensile stress would be on the order of 30 ksi. Based on the FEA and depending on the number of threads sharing the load, it is not un-reasonable for tensile stresses to range from approximately 20 ksi to 80 ksi at the thread root.

3.5 SCC Growth Evaluation

The time to failure of a susceptible material in a given environment is dependent on the applied tensile stress, as can be seen in Figure 3-7. The plot compares applied stress or load to the logarithm of exposure time in an

[4] Based on extensive testing, as presented in various literature sources [9], the threads nearest the plane of load application carry the majority of the applied loading.

environment and illustrates the time to failure increases significantly with decreasing applied stress. The crack propagation time, t_{cp} is taken to be the difference between the time of failure, t_f, minus the time of initiation, t_{in}. The time at failure is typically known. However, the time of initiation is highly alloy-environment and applied stress dependant and thus is an unknown without specific test data. The initiation time is also highly dependent upon pre-existing flaws that may have been introduced during heat treatment or thread fabrication. Therefore, predicting initiation time is difficult. Unless there are preexisting flaws, a distribution of 80% initiation and 20% propagation is considered reasonable for the life of a component subject to SCC process as suggested by Figure 3-8.

The SCC process usually occurs in three stages:

1) crack initiation and stage 1 propagation,
2) stage 2 or steady-state propagation (independent of stress intensity), and
3) stage 3 crack propagation or final fracture.

A typical plot of crack growth rate (da/dt) versus stress intensity illustrating the three stages of SCC propagation is presented in Figure 3-9. The figure illustrates a threshold stress-intensity, K_{1SCC}, for SCC initiation and stage 1 propagation. The threshold stress-intensity is dependent upon interaction of the alloy and environment (alloy-environment). Stage 1 propagation is followed by Stage 2 crack propagation where the crack growth velocity is independent of stress intensity. Stage 2 crack growth velocity is limited to the alloy-environment interaction such as the mass transfer of corrosive environmental elements up the crack to the crack tip. Stage 3 propagation is dependent upon stress intensity, until the critical level, K_{1c} to produce mechanical overload of the remaining ligament. The crack propagation time is the sum of the time at each stage, $t_{cp}=t_1+ t_2+ t_3$.

A plot of crack growth rate (da/dt) versus stress intensity for 12% chromium and 0.2% carbon alloy at various tempering temperature per [7] is provided in Figure 3-10. The generic categorization of 12% Cr and 0.2% C would cover the 416 SS coupling material. Based on tempering heat traces for the P-7A and P-7B couplings presented in Figure 3-11, the 550°C (1022°F) curve is appropriate. Figure 3-10 show that the threshold stress-intensity, K_{1SCC} for the 550°C curve is approximately $20Mpa\sqrt{m}$ ($\sim 18ksi\sqrt{in}$) and the stage 2, stress intensity independent crack growth rate is approximately 2.3E-4 in/hr per [7].

For a stress distribution of 20 to 80 ksi, the stress intensity at the thread root (without pits) of the coupling can range from $6ksi\sqrt{in}$ to $26ksi\sqrt{in}$ as demonstrated below.

$j := 0..3$

$d_{thread} = 0.068\,in$ Thread height

$a := \frac{d_{thread}}{2}$ $a = 0.034in$ Load assumed to act at center of threads.

$\sigma_j :=$ $K_j := \sigma_j \cdot \sqrt{\pi \cdot a}$ [14] $K_j =$

σ_j	K_j (ksi·$\sqrt{in}$)
20ksi	6.5
55ksi	17.9
70ksi	22.8
80ksi	26.1

Therefore, based on three threads taking the load and resulting tensile stress of 70 ksi (see Figure 3-6), the stress intensity of $23ksi\sqrt{in}$ would be sufficient to initiate a crack. If the tensile stress at the thread root is 55 ksi or less then the stress intensity would fall below the threshold stress intensity, K_{1SCC} of $18ksi\sqrt{in}$ and SCC initiation would not be expected. However, if a pit were to form at the thread root, the stress intensity would be higher for a given tensile stress. For example, a pit 0.01" deep and tensile stress of 55 ksi would result in a stress intensity of approximately $24ksi\sqrt{in}$ (see below), which is greater than the threshold stress intensity for SCC initiation.

$Q := 0.9$ $M := 1$

$d_{pit} := 0.01in$ Assumed pit depth

$a := d_{pit} + a$ $a = 0.044in$

$\sigma_j :=$ $K_j := 1.12\,\sigma_j \cdot \sqrt{\frac{\pi \cdot a}{Q}} \cdot M$ [14] $K_j =$

σ_j	K_j (ksi·$\sqrt{in}$)
20ksi	8.8
55ksi	24.1
70ksi	30.7
80ksi	35

Once a crack initiates, the stress intensity would increase with increasing crack length, however the crack rate is limited to the stage 2 propagation rate until the critical fracture stress intensity, K_{1c} resulting in failure by overload.

To determine whether the couplings extracted from P-7A and P-7B would have survived a mission time of 30 days, an appropriate crack growth rate (CGR) is required. The following three cases evaluates crack growth rates based the life of failed couplings 09-P7C-7F and 11-P7C-6F and the stress intensity independent crack growth rate from Figure 3-10.

Case 1 – CGR based on Figure 3-10

Using the stage 2 stress intensity independent crack growth rate (CGR) of 2.3E-4 in/hr from Figure 3-10, and applying it to the as-found cracks of examined couplings from P-7B, it would require approximately 66 days to propagate through the wall[5] of the deepest flaw found on the P-7B couplings, i.e. 11-P7B-6K (evaluation is shown in Figure 3-12). Using the same CGR, and assuming a crack initiated at the time the examined P-7A couplings were removed from service, it would require 90 days to propagate through wall. Applying this simplistic approach to couplings 09-P7C-7F and 11-P7C-6F would result in the same 90 days to propagate through thickness (see Figure 3-12).

Based on the loading mechanism discussed in Section 3.4, coupling tensile stress would be generated at pump start-up following coupling assembly and is independent of pump starts and stops. Therefore coupling life is based upon the time of installation. Using the 90 days of propagation life, the initiation time would be approximately 19 days for coupling 09-P7C-7F and 586 days for 11-P7C-6F (see Figure 3-12).

It is apparent that there is quite a disparity between initiation time and life of these two couplings. That is, the initiation time of 09-P7C-7F comprise only 17% of its life whereas the initiation time of 11-P7C-6F is 87%. The disparity could be explained by differences between impact energy test results (3 to 4 ft-lb for 09-P7C-7F vs. 6 to 8 ft-lb for 11-P7C-6F at 32°F) and/or stress levels and/or a preexisting flaw in 09-P7C-7F. A preexisting flaw combined with the low impact energy in 09-P7C-7F, would result in

[5] Examination of the fracture surface of coupling 11-P7C-6F in [3] indicates SCC propagation through wall prior to final overload.

a shorter initiation time. Also, based purely on the concept provided in Figure 3-7, coupling 09-P7C-7F would have been subjected to higher stresses than 11-P7C-6F to produce the initiation time disparity.

Case 2 – CGR based on 50/50 Life Split of 09-P7C-7F

Assuming a 50/50 split for initiation and propagation in the life of coupling 09-P7C-7F would result in a propagation rate of about 3.81E-4 in/hr. Applying a propagation rate of 3.81E-4 in/hr to the examined couplings would result in an initiation time of about 622 days and propagation time of 55 day for 11-P7C-6F (see below). Since SCC propagation rate is alloy-environment dependant and stress independent in stage 2 (plateau velocity), applying the same crack velocity to the SWS pump coupling is considerable reasonable. Using a CGR of 3.81E-4 in/hr would result in initiation making up 92% of the life of coupling 11-P7C-6F.

Initiation time is taken to be the elasped time from installation minus the propagation tme.

$$T_{init_i} := IT_i - T_{prop_i}$$

$$\%InitLife_i := \frac{T_{init_i}}{IT_i}$$ Percentage of initiation to total life

	T_{init} = (day)	T_{prop} = (day)	%InitLife = (%)
<-- 09-P7C-7F-->	55	55	50
<-- 11-P7C-6F -->	622	55	92
<-- 11-P7C-7K -->	662	14	98
<-- 11-P7B-5K -->	468	7	99
<-- 11-P7B-6K -->	460	14	97
<-- 11-P7B-7K -->	470	5	99
<-- 11-P7A -->	876	0	100

Case 3 – CGR based on 0/100 Life Split of 09-P7C-7F

Assuming a preexisting flaw and propagation life to be the total life of coupling 09-P7C-7F would result in a CGR of about 1.91E-4 in/hr. Applying this propagation rate to coupling 11-P7C-6F would result in an initiation life about 84% of the total life. This CGR results in reasonable initiation and propagation distribution for failed coupling 11-P7C-6F and the cracked couplings, as shown below.

Initiation time is taken to be the elasped time from installation minus the propagation tme.

$$T_{init_i} := IT_i - T_{prop_i}$$

$$\%InitLife_i := \frac{T_{init_i}}{IT_i}$$ Percentage of initiation to total life

$$T_{init} = \begin{pmatrix} 0 \\ 567 \\ 649 \\ 460 \\ 446 \\ 465 \\ 876 \end{pmatrix} day \qquad \begin{matrix} \text{<-- 09-P7C-7F-->} \\ \text{<-- 11-P7C-6F -->} \\ \text{<-- 11-P7C-7K -->} \\ \text{<-- 11-P7B-5K -->} \\ \text{<-- 11-P7B-6K -->} \\ \text{<-- 11-P7B-7K -->} \\ \text{<-- 11-P7A -->} \end{matrix} \qquad T_{prop} = \begin{pmatrix} 109 \\ 109 \\ 27 \\ 14 \\ 29 \\ 9 \\ 0 \end{pmatrix} day \qquad \%InitLife = \begin{pmatrix} 0 \\ 84 \\ 96 \\ 97 \\ 94 \\ 98 \\ 100 \end{pmatrix} \%$$

Case	Coupling	Life (days)	CGR (in/hr)	Initiation (days)	Propagation (days)	Init/Life (%)
1	09-P7C-7F	110	2.3E-4	19	90	17%
	11-P7C-6F	676	2.3E-4	586	90	87%
2	09-P7C-7F	110	3.81E-4	55	55	50%
	11-P7C-6F	676	3.81E-4	621	55	92%
3	09-P7C-7F	110	1.91E-4	0	110	0%
	11-P7C-6F	676	1.91E-4	566	110	84%

Note(s)

1. Life is based on time of installation.
2. CGR = Crack Growth Rate

Based on the above assessment, a reasonable crack growth rate for the SWS pump couplings is in the range of 1.91E-4 in/hr to 3.81E-4 in/hr. This range encompasses the stress intensity independent CGR of 2.3E-4 in/hr for 12%Cr, 0.5%C steel tempered at 550°C in distilled water per [7] (see Figure 3-10). However, the CGR of 1.91E-4 in/hr is the most reasonable in terms of initiation and propagation distribution life for failed coupling 11-P7C-6F and all cracked couplings. This means that coupling 09-P7C-7F is anomalous (e.g. preexisting flaw) and is postulated to have propagated shortly after installation. Barring specific CGR for the alloy-environment interaction of the SWS pump couplings, using a CGR of 2.3E-4 in/hr is considered as a reasonable mean value and 3.81E-4 in/hr is considered a bounding value for this evaluation.

4.0 SUMMARY

Pump shaft couplings from PLP SWS Pumps P-7A and P-7B were submitted to LPI for examination and metallurgical testing. Examination of the couplings revealed cracks in couplings 5, 6 and 7 (these are subjected to wet/dry cycles) from pump P-7B, but cracks were not observed in examined P-7A couplings.

Visual examination of couplings 4 through 7 from pump P-7A identified them to be well coated with Neolube to a greater degree than on examined P-7B and P-7C couplings. Very little to none was observed on couplings 11-P7C-6F and 11-P7C-7K. It is postulated that the presence of liberal amounts of Neolube on the threads of examined P-7A couplings enhanced its pitting resistance by providing a coating that protected the thread roots from corrosive agents in the service water basin environment.

Considering the coupling material and environment, a stress intensity, K independent crack growth rate (CGR) of 3.81E-4 in/hr is considered a reasonable bounding value for this evaluation. This CGR encompasses the stress intensity independent CGR of 2.3E-4 in/hr for 12%Cr, 0.5%C steel tempered at 550°C (1022°F) in distilled water per [7] (see Figure 3-10). Using a CGR of 3.81E-4 in/hr, in conjunction with the as-found flaws on the P-7B couplings, it would require approximately 40 days to propagate through the wall for the deepest flaw found on coupling 11-P7B-6K. Since no flaws were found on examined P-7A couplings, it is concluded that it would require approximately 54 days for a flaw to propagate through wall if, conservatively, a crack initiated at the time they were removed from service. Also since pits are a precursor to cracks (as observed on the examined P-7B and P-7C couplings that exhibit cracks) and no cracks were found on the examined P-7A coupling, it is postulated that the life of examined couplings extracted from P-7A could be greater than 54 days to allow for pit formation.

LPI concludes that the couplings removed from service water pump P-7A and P-7B would have continued to perform their design function for at least an additional 30 days of operation from the time of extraction.

5.0 REFERENCES

1. PLP Condition Report Entergy Palisades Root Cause Evaluation for CR-PLP-2009-04519, "Service Water Pump P-7C Failure to Provide Discharge Pressure" 3/4/2010, Rev. 1
2. Entergy Palisades Root Cause Evaluation Report for CR-PLP-2011-03902, "Service Water Pump 7-C Line Shaft Coupling Failure"
3. LPI Report No. F11358-R-001, Rev. Draft G, "Metallurgical and Failure Analysis of SWS Pump P-7C Coupling #6"
4. PLP Maintenance Procedure WI-SWS-M-03 and WI-SWS-M-04.
5. PLP Response to NRC RFI # 43 "Operating Service History Since Last Coupling Failure"
6. Entergy Contract No. 10325528
7. M.O. Speidel "Corrosion Fatigue in Fe-Ni-Cr Alloys", NACE-5 Stress Corrosion Cracking and Hydrogen Embrittlement of Iron Base Alloys, National Association of Corrosion Engineers, Houston, 1977, p. 1071 to 1094.
8. ASM Handbook, Volume 13A "Stress-Corrosion Cracking", R.H. Jones, Battelle Pacific Northwest National Laboratory.
9. Pilkey, Walter "Peterson's Stress Concentration Factors", 2nd Edition,. © 1997 John Wiley & Sons
10. API 579-1/ASME FFS-1- Fitness-for Service, API/ASME 2007
11. OBERG E, et al. "Machinery's Handbook" 25th Ed. Industrial Press
12. HydroAire Calculation NQ5940, "Maximum combined shear stress calculation for threaded coupling", Rev. 3
13. ASM Handbook, Volume 13A "Evaluating Stress-Corrosion Cracking", S.D. Cramer, B.S. Covino, Jr, Revised by Bopinder Phull.
14. R.W. Hertzberg, "Deformation and Fracture Mechanics of Engineering Materials", 2nd Edition John Wiley & Sons.
15. ANSYS Inc., LPI Report No. V&V-ANSYS-11, Rev. 3,"Verification and Validation of ANSYS Software Program"

6.0 QUALITY ASSURANCE

The outlined work has been performed in accordance with the requirements of Entergy Purchase Order 10325528 [6]. The Approver of this document attests that all project examinations, inspections, tests and analysis (as applicable) have been conducted using approved LPI Procedures and are in conformance to the contract/purchase order. Ref. 3 is in draft form at this time, but does not impact the conclusions reached in this letter report, relative to estimated life of extracted couplings from pump P-7A and P-7B.

Rev	Date	Prepared	Checked	Design Verified	Approved
0	9/28/11	[signature]	[signature]	[signature] G. Zysk	[signature]
		S. Yim	J. Mills, Ph.D.	G. Zysk	P. Bruck

Table 2-1: CVN IMPACT TEST RESULTS					
Coupling	Specimen Identification	Test Temperature (°F)	Absorbed Energy (ft-lb)	Lateral Expansion (in.)	Percent Shear (%)
11-P7A-5	5-A3	32	7	0.003	<10
	5-A4	32	7	0.002	<10
	5-A1	75	8	0.006	10
	5-A2	75	9	0.005	10
	5-A5	100	13	0.009	30
11-P7A-6	6-A3	32	3	0.002	<10
	6-A4	32	3	0.002	<10
	6-A1	75	6	0.006	10
	6-A2	75	6	0.008	10
	6-A5	100	9	0.012	10
11-P7A-7	7-A3	32	11	0.005	<10
	7-A4	32	9	0.004	<10
	7-A1	75	12	0.009	20
	7-A2	75	12	0.010	20
	7-A5	100	18	0.015	50
11-P7B-5	B5-9	0	9	0.006	10
	B5-10	0	10	0.007	10
	B5-1	32	14	0.013	20
	B5-2	32	16	0.014	40
	B5-7	32	12.5	0.011	20
	B5-8	32	13	0.011	20
	B5-3	76	22	0.018	>90
	B5-4	76	29	0.018	>90
	B5-5	100	28	0.016	>90
	B5-6	150	26	0.017	>90
11-P7B-6	B6-9	0	5	0.004	<10
	B6-10	0	5	0.004	<10
	B6-1	32	8	0.004	<10
	B6-2	32	5	0.005	<10
	B6-7	32	6	0.005	<10
	B6-8	32	6	0.003	<10
	B6-3	76	11	0.008	10

Mr. Alan Blind
LPI Ref. F11358-LR-001, Rev. 0

Table 2-1: CVN IMPACT TEST RESULTS

Coupling	Specimen Identification	Test Temperature (°F)	Absorbed Energy (ft-lb)	Lateral Expansion (in.)	Percent Shear (%)
	B6-4	76	10	0.009	10
	B6-5	100	21	0.015	80
	B6-6	150	21	0.015	>90
	B7-9	0	8	0.007	10
	B7-10	0	9	0.007	10
	B7-1	32	12	0.008	20
	B7-2	32	11	0.009	20
	B7-7	32	11	0.009	10
	B7-8	32	14	0.013	20
	B7-3	76	11	0.015	50
	B7-5	100	22	0.016	>90
11-P7B-7	B7-6	150	32	0.022	>90

Table 2-2: TENSILE TEST RESULTS

Coupling	Specimen Identification	Yield Strength (ksi)	Tensile Strength (ksi)	Elongation (%)
11-P7A-5	5-1	131.8	146.1	14.1
	5-2	136.0	152.6	14.6
11-P7A-6	6-1	111.5	126.3	16.2
	6-2	108.1	123.2	16.1
11-P7A-7	7-1	136.3	150.5	12.8
	7-2	135.9	150.2	15.4
	5-1	117.5	135.6	17.9
11-P7B-5	5-2	117.7	135.6	14.6
	6-1	130.5	143.8	14.2
11-P7B-6	6-2	126.1	139.6	15.2
	7-1	114.2	129.3	17.3
11-P7B-7	7-2	114.5	129.1	16.5

Table 2-3: COMPOSITION OF COUPLINGS (WT%)

Element	Coupling			ASTM A582 [7]
	11-P7A-5	11-P7A-6	11-P7A-7	
C	0.14	0.10	0.13	0.15 max
Cr	13.06	12.16	12.97	12.00 – 14.00
Cu	0.071	0.077	0.073	ns
Mn	0.74	0.83	0.65	1.25 max
Mo	0.07	0.12	0.06	0.60 max
Ni	0.22	0.43	0.22	ns
P	0.018	0.021	0.017	0.060 max
S	0.35	0.22	0.35	0.15 min
Si	0.42	0.34	0.42	1.00 max

ns – not specified

Element	Coupling			ASTM A582
	11-P7B-5	11-P7B-6	11-P7B-7	
C	0.13	0.12	0.12	0.15 max
Cr	12.1	12.0	12.0	12.00 – 14.00
Cu	0.082	0.079	0.078	ns
Mn	0.72	0.70	0.72	1.25 max
Mo	0.080	0.078	0.078	0.60 max
Ni	0.28	0.27	0.27	ns
P	0.02	0.02	0.02	0.060 max
S	0.37	0.29	0.34	0.15 min
Si	0.37	0.37	0.37	1.00 max

Table 2-4: SURFACE HARDNESS OF COUPLINGS

Coupling	End	Average (HRC)	Measurements (HRC)
11-P7A-5	top	32.5	32.5, 32.0, 32.5, 32.0, 33.0, 33.0
	bottom	29.9	28.0, 31.5, 31.5, 30.0, 30.5, 28.0
11-P7A-6	top	25.3	25.5, 25.5, 25.0, 25.5, 25.0, 25.5
	bottom	23.8	24.5, 23.5, 23.5, 25.0, 22.0, 24.0
11-P7A-7	top	31.5	31.0, 31.5, 32.0, 32.0, 32.5, 31.0
	bottom	28.7	28.0, 28.0, 27.0, 30.0, 29.0, 30.0
11-P7B-5	top	27.6	28.0, 28.0, 27.5, 28.5, 26.5, 27.0
	bottom	26.1	25.0, 27.0, 26.5, 25.0, 27.0, 26.0
11-P7B-6	top	29.9	30.0, 30.0, 30.5, 30.0, 30.0, 29.0
	bottom	28.5	27.5, 29.0, 28.0, 28.5, 28.5, 29.5
11-P7B-7	top	28.3	28.0, 28.0, 28.5, 29.0, 28.5, 28.0
	bottom	26.1	25.5, 27.0, 26.0, 27.0, 24.5, 26.5

Table 2-5: THROUGH THICKNESS HARDNESS OF COUPLINGS

Coupling	Location	Measurements from OD to ID (HRC)
11-P7A-5	1	33.0, 29.9, 33.2, 33.0, 33.6, 32.2
	2	32.9, 32.9, 33.0, 32.6, 32.8, 33.1
11-P7A-6	1	24.0, 24.0, 24.0, 24.0, 24.0, 24.0
	2	24.5, 24.0, 24.0, 24.0, 24.5, 24.0
11-P7A-7	1	31.0, 31.5, 31.0, 31.5, 31.0, 31.0
	2	32.0, 31.5, 32.0, 31.0, 31.0, 31.0
11-P7B-5	1	27.0, 27.5, 27.5, 28.0, 27.9, 27.5
	2	28.5, 28.0, 28.6, 28.0, 27.7, 28.1
11-P7B-6	1	28.8, 29.0, 29.1, 29.4, 29.8, 29.8
	2	29.2, 29.9, 30.0, 30.0, 30.1, 30.2
11-P7B-7	1	28.2, 28.0, 27.9, 27.9, 28.0, 28.5
	2	28.1, 28.8, 28.7, 28.5, 28.4, 28.6

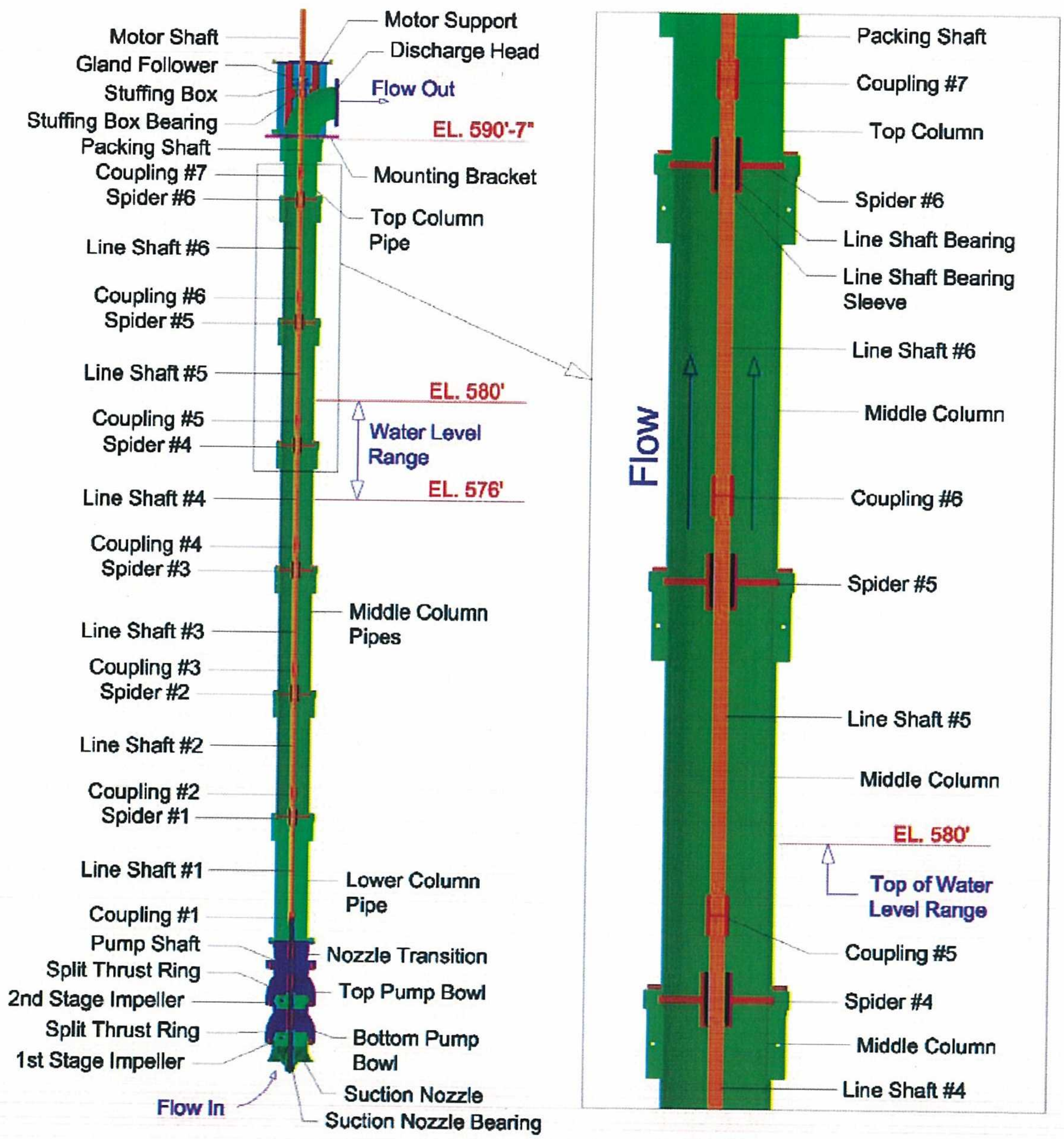

Figure 1-1: SWS Pump Sketch

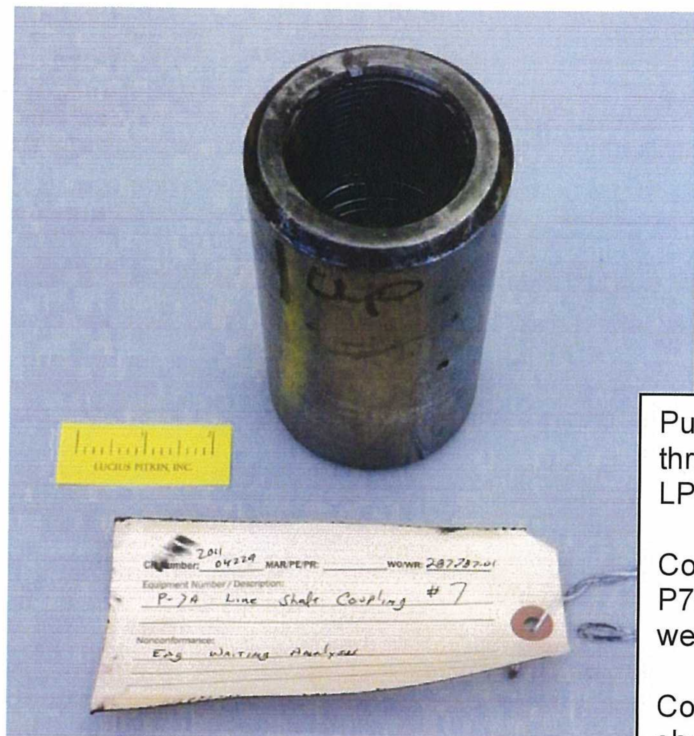

Pump P-7A Coupling No. 1 through 8 were submitted to LPI.

Coupling Nos. 5, 6 and 7 (11-P7A-5, 11-P7A-6, 11-P7A-7) were selected for analysis

Coupling No. 7 (11-P7A-7) shown in its as-received condition.

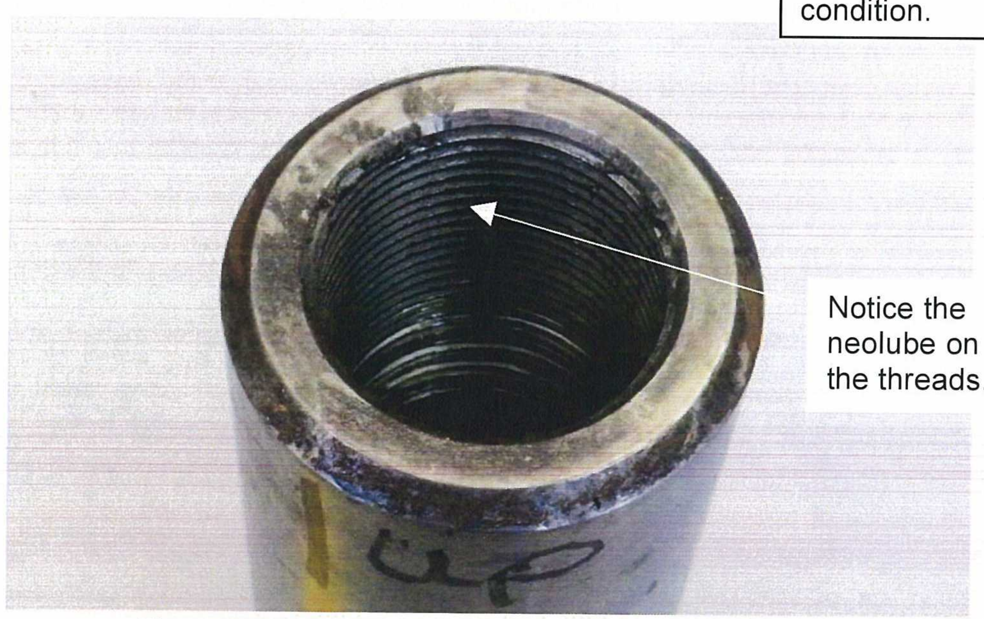

Figure 2-1: As-Received Coupling No. 11-P7A-7

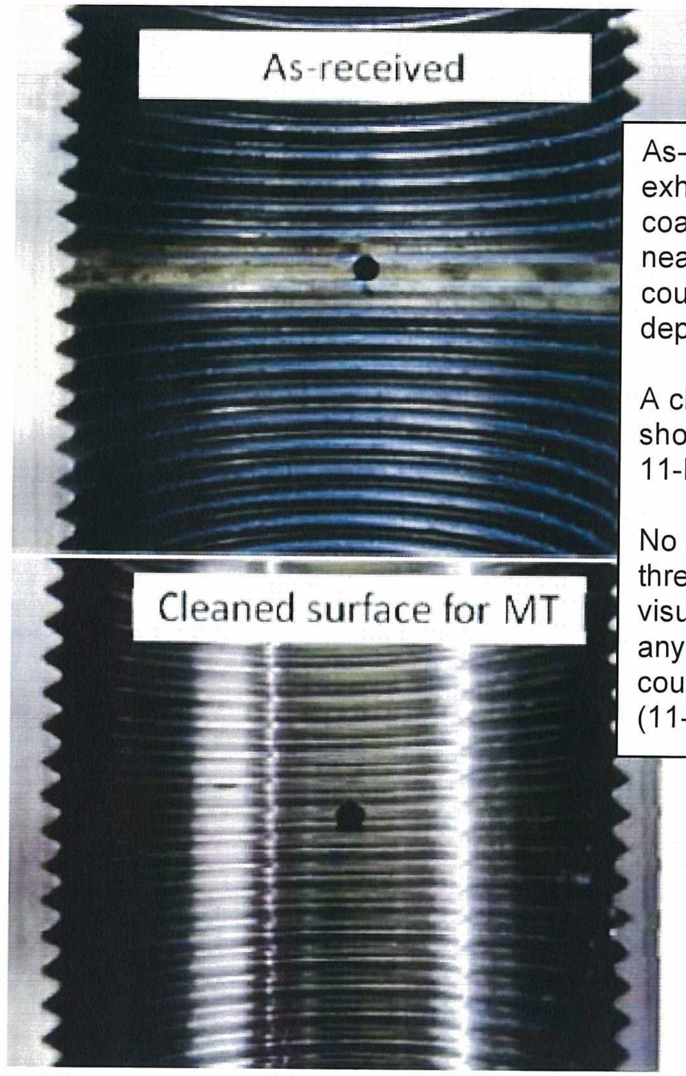

As-received couplings exhibited a greasy grey coating on threads, and near the center of the coupling some surface deposits.

A cleaned surface is shown for coupling No. 11-P7A-5

No cracks along the thread root were visually observed for any of the cleaned couplings (11-P7A-4, 5, 6, 7)

Figure 2-2: Visual Observation of Coupling No. 11-P7A-5

Pump P-7A coupling Nos. 11-P7A-5, 6, 7 were sectioned longitudinally, as shown in the figure.

The threaded inner diameter region of couplings nos. 11-P7A-4, 5, 6, and 7 were examined for cracks or discontinuities by fluorescent magnetic particle testing (MT)

No indications were readily visible in these couplings

Figure 2-3: MT Examination of Coupling No. 11-P7A-6

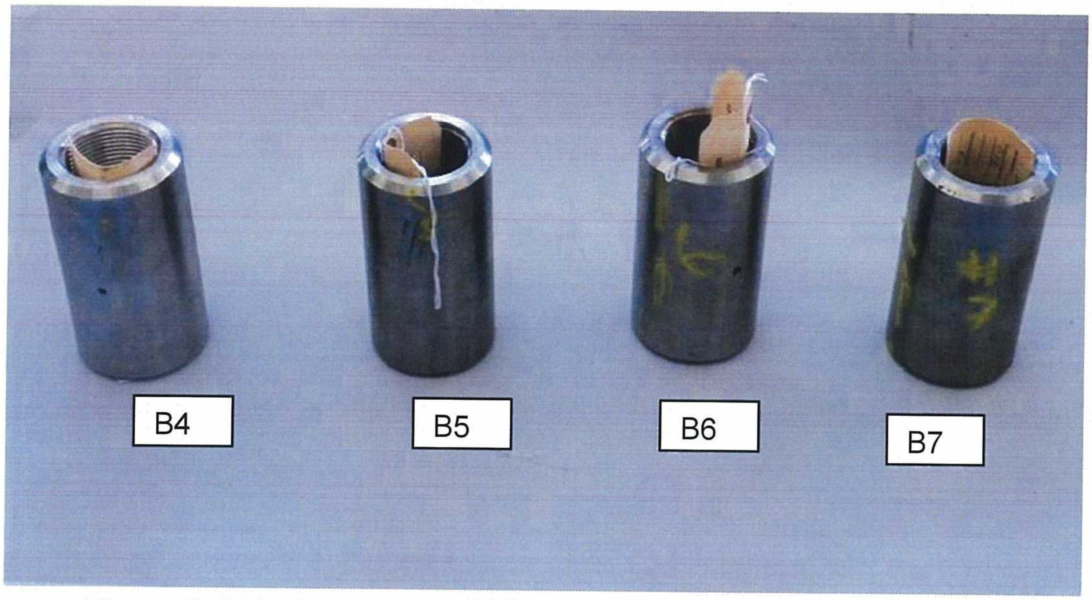

Figure 2-4: As-Received Couplings 11-P7B-4 through 11-P7B-7

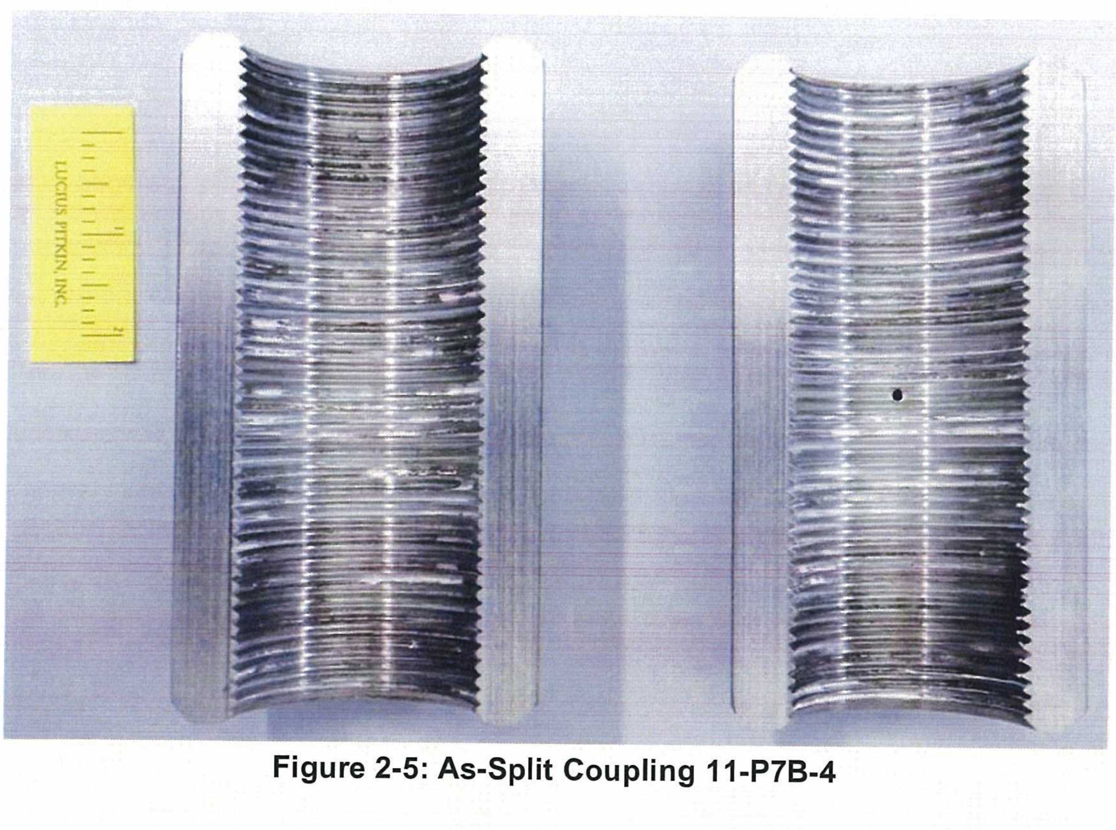

Figure 2-5: As-Split Coupling 11-P7B-4

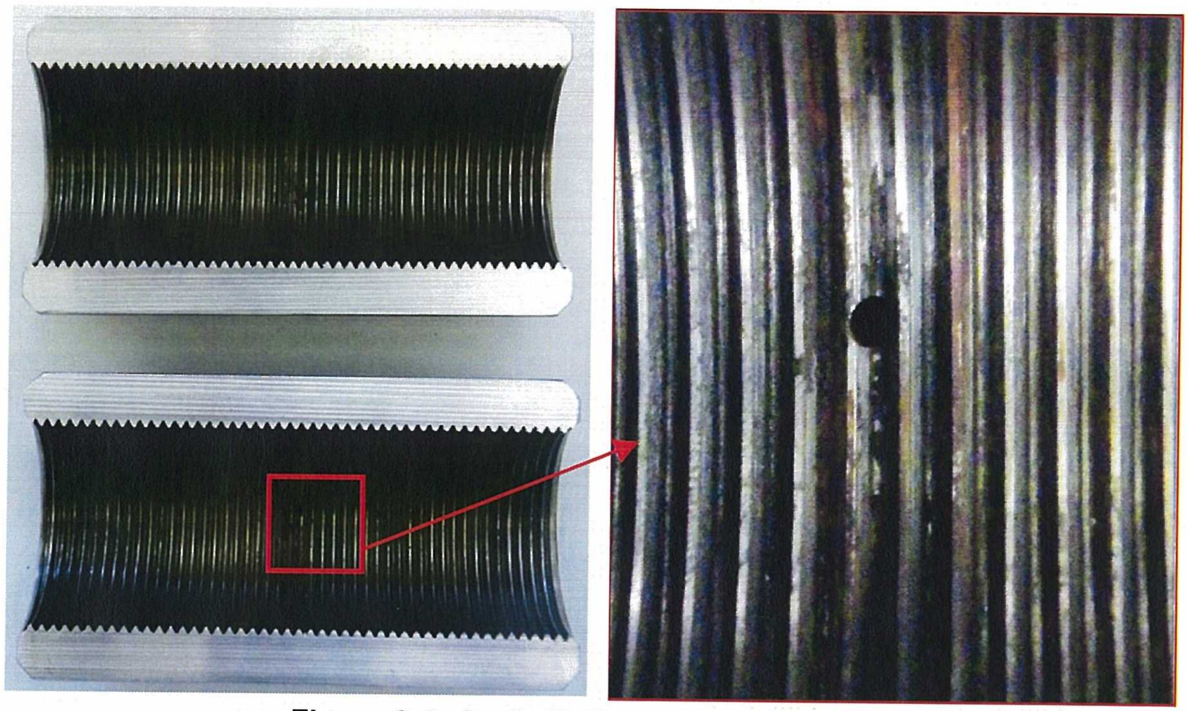

Figure 2-6: As-Split Coupling 11-P7B-5

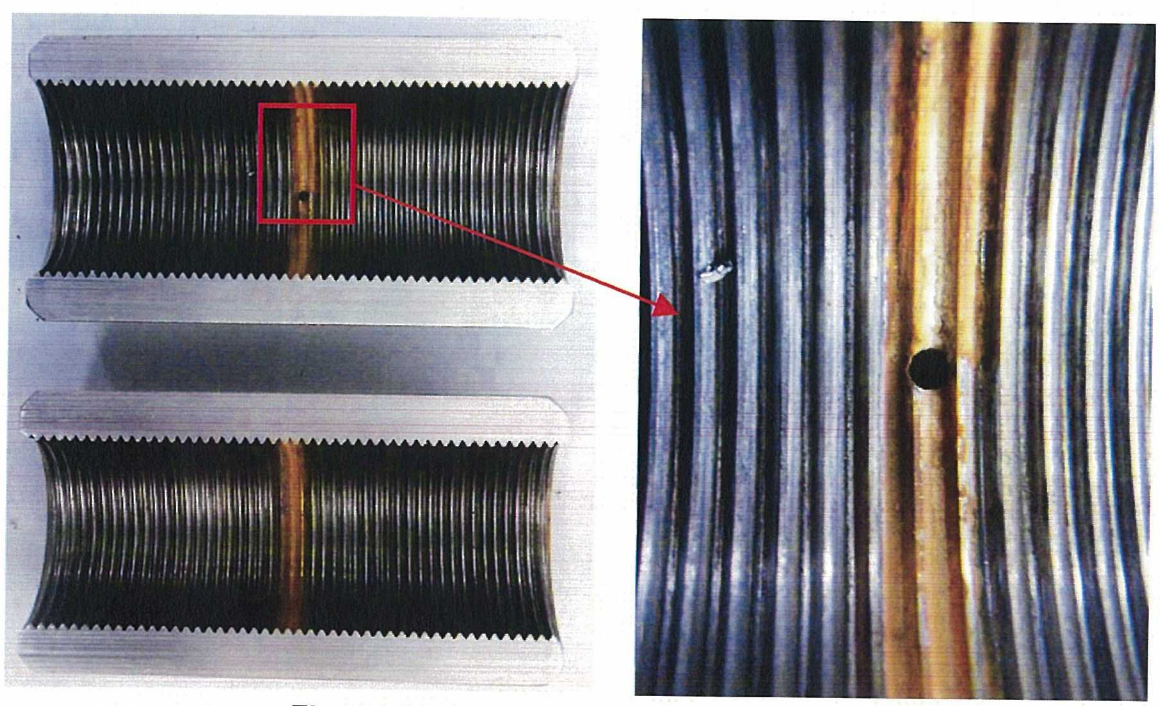

Figure 2-7: As-Split Coupling 11-P7B-6

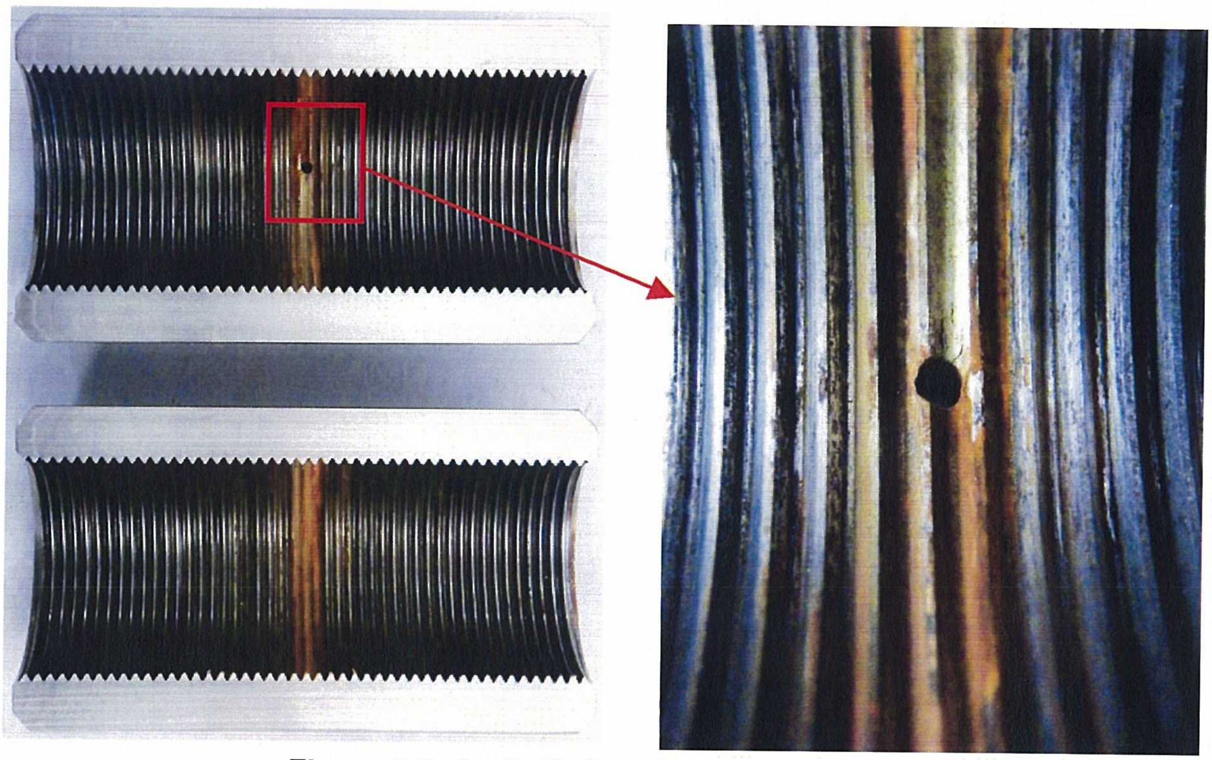

Figure 2-8: As-Split Coupling 11-P7B-7

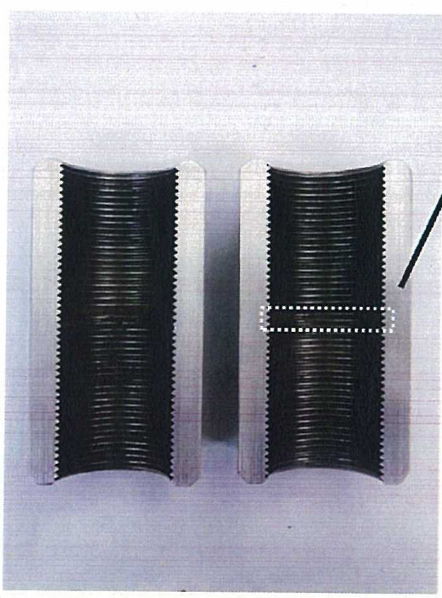

Coupling split longitudinally

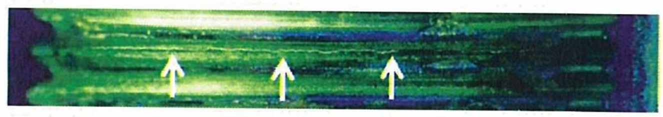

Fluorescent MT reveals an indication 1.5 in. long at the center of the coupling

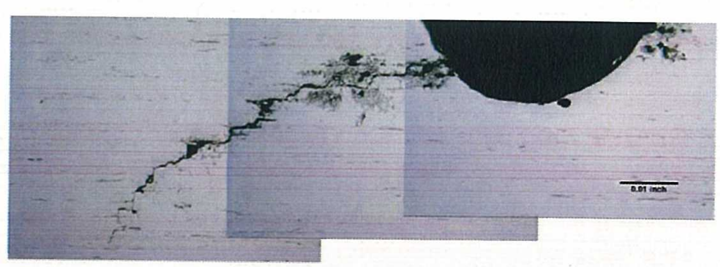

Network of cracks, characteristic of SCC, originating at thread root, as shown in the cross-sectional view. Evidence of pitting at surface of thread. (As-polished, 100X, scale bar 0.01 in.)

Figure 2-9: Cracks in 11-P7B-5 Initiating at a Pit

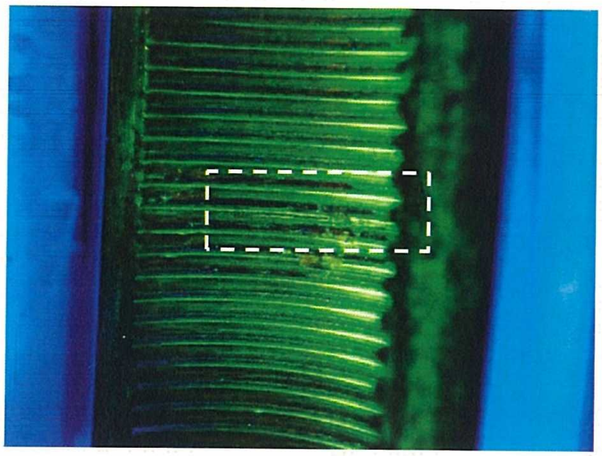

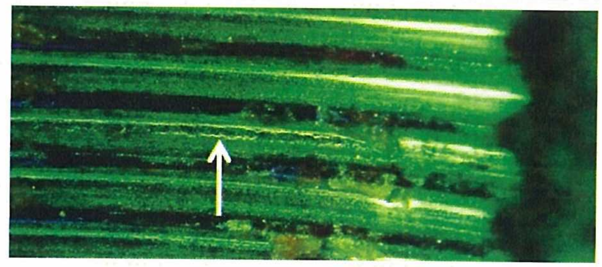

0.5 in. long indication found at center of Coupling No. 6

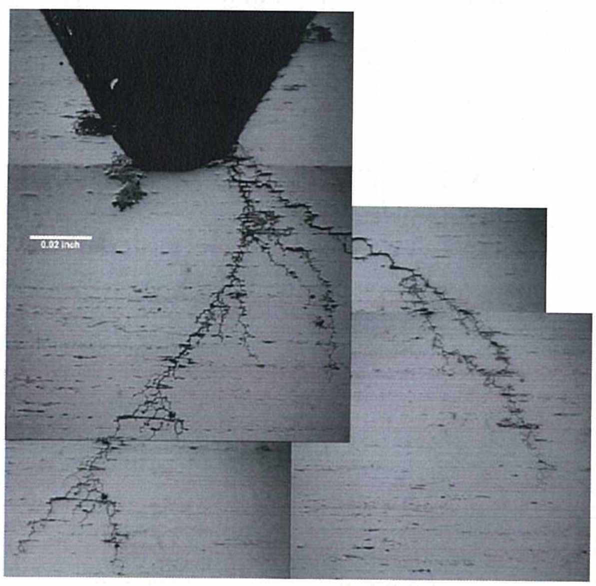

Network of cracks, characteristic of SCC, originating at thread root. Evidence of pitting at surface of thread. (As-polished, 50X, scale bar 0.02 in.)

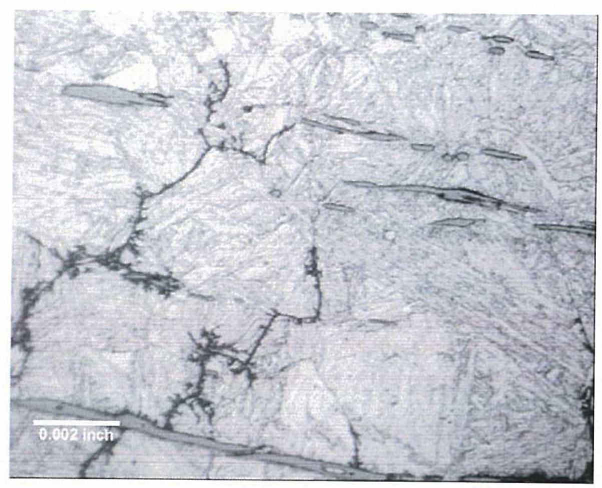

Path of networked cracks along grain boundaries. (Etched, 400X, scale bar 0.002 in.)

Figure 2-10: Cracks in 11-P7B-6 Initiating at a Pit

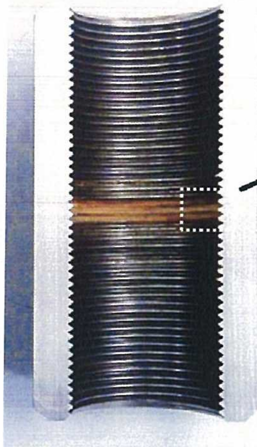

Coupling split longitudinally

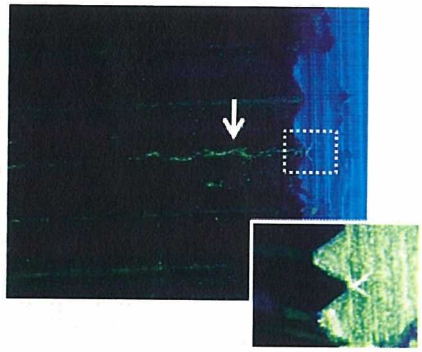

Fluorescent MT reveals an indication 0.5 in. long at the center of the coupling

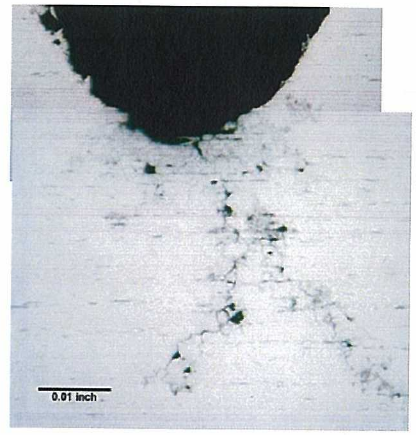

Network of cracks, characteristic of SCC, originating at thread root, as shown in the cross-sectional view. Evidence of pitting at surface of thread. (As-polished, 100X, scale bar 0.01 in.)

Figure 2-11: Cracks in 11-P7B-7 Initiating at a Pit

Sontra Yim

From:	DeBusscher, Derek [ddebuss@entergy.com]
Sent:	Wednesday, September 28, 2011 8:02 AM
To:	Sontra Yim
Cc:	Forehand, James M
Subject:	RE: Palisades comments on LPI report F11358-LR-001
Attachments:	RFI 43 Response.doc

Sontra,

P-7B was put into service with the new couplings on 5/12/10 as stated by the WO 20082. From that date I calculated the approximate run time hours to be 9072.5 and the pump start/stops to be 70 since that time. Total installed hours are approximated 11,391 hrs.

I have attached the RFI that was reviewed. Note that the times only include up to 8/9/11. P-7B ran for 703 hrs during August (not 204), and had one additional start.

If there is any other information you need please let me know so we can get this minor issue hashed out as soon as possible.

Thanks.

Derek DeBusscher
BOP Systems Engineering
Palisades Nuclear Power Plant
269-764-2997
ddebuss@entergy.com

Figure 3-0: P-7B Run Time

Data Source: Palisades PI Datalink

Time Start: **6/12/09 0:00**
Time Stop: **10/1/09 0:00**

Update highlighted cells and click "Update Sheet" button.

Update Sheet (must have PI add-in installed)

	Service Water Pump P-7C		**None**	**None**
Total Run Time:	**2414.44**	**hrs**		
1	6/12/09 12:22 6/12/09 12:23	Started Stopped		
2	6/12/09 15:03 6/12/09 15:33	Started Stopped		
3	6/12/09 15:34 6/19/09 3:44	Started Stopped		
4	6/19/09 16:17 7/17/09 10:52	Started Stopped		
5	7/17/09 11:42 7/17/09 12:02	Started Stopped		
6	7/17/09 13:22 7/23/09 5:03	Started Stopped		
7	7/23/09 9:04 8/8/09 21:38	Started Stopped		
8	8/8/09 21:39 8/13/09 3:55	Started Stopped		
9	8/13/09 3:56 8/28/09 10:40	Started Stopped		
10	8/28/09 10:41 9/2/09 13:06	Started Stopped		
11	9/9/09 11:15 9/22/09 20:32	Started Stopped		
12	9/22/09 23:38 9/29/09 7:34	Started Stopped		
13	9/29/09 7:35 9/29/09 9:11	Started Stopped		
14				

Figure 3-1: P-7C Run Time

Coupling No. 11-P7C-6F

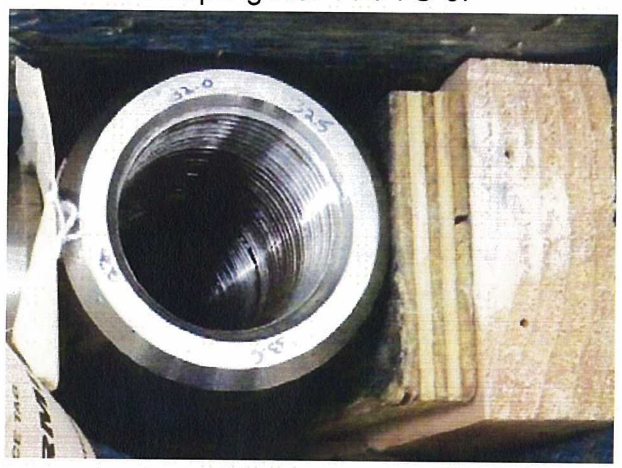

11-P7C-7K in the as-received condition does not exhibit the same level of neolube on threaded surface as 11-P7A-7

11-P7A-7 in the as-received condition exhibits significant amounts of neolube on thread surface

Figure 3-2: Contrast Thread Coating (As-Received) on P-7C Failed and Cracked Couplings to P-7A Coupling

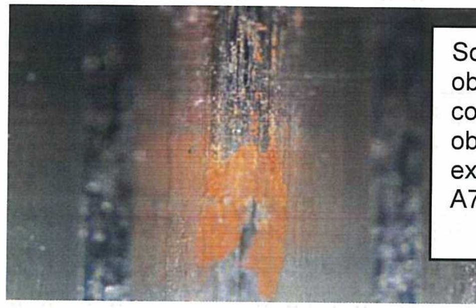

Some corrosion product was observed near the middle of the coupling however no pitting was observed during stereomicroscope examination of couplings A5 through A7.

Representative Image of 11-P7A Coupling

Pitting near root at middle of Coupling No. 5 (Stereomicroscopy 40X)

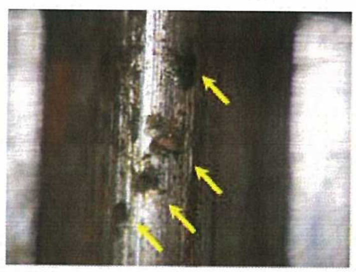

Pitting at root near middle of Coupling No. 6 (Stereomicroscopy 50X)

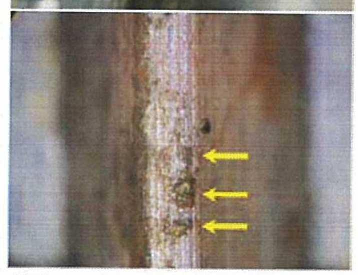

Pitting at root near middle of Coupling No. 7 (Stereomicroscopy 50X)

11-P7B Couplings

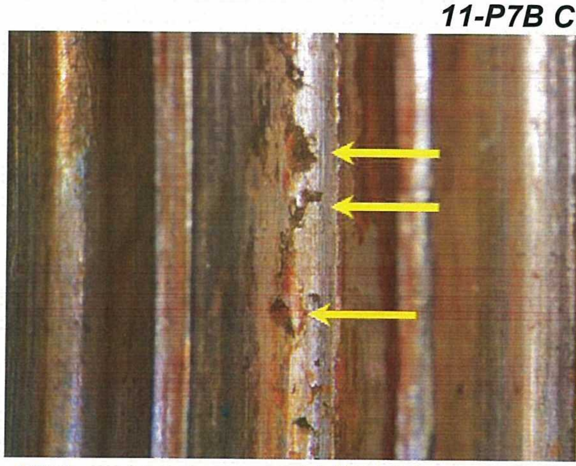

Pitting at root near middle of fractured Coupling No. 6 (Stereomicroscopy 15X)

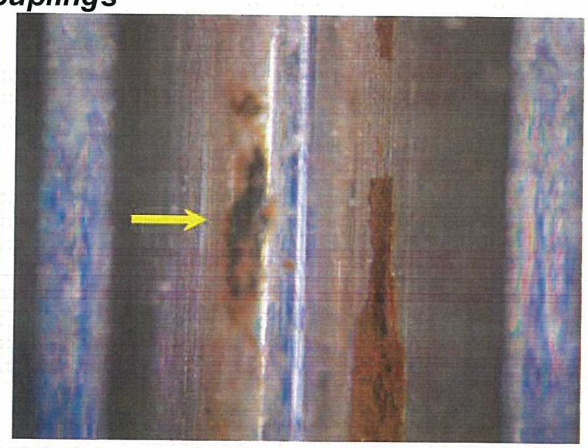

Pitting near the root and near middle of Coupling No. 7 (Stereomicroscopy 40X)

11-P7C Couplings

Figure 3-3: Contrast Thread Root Pitting

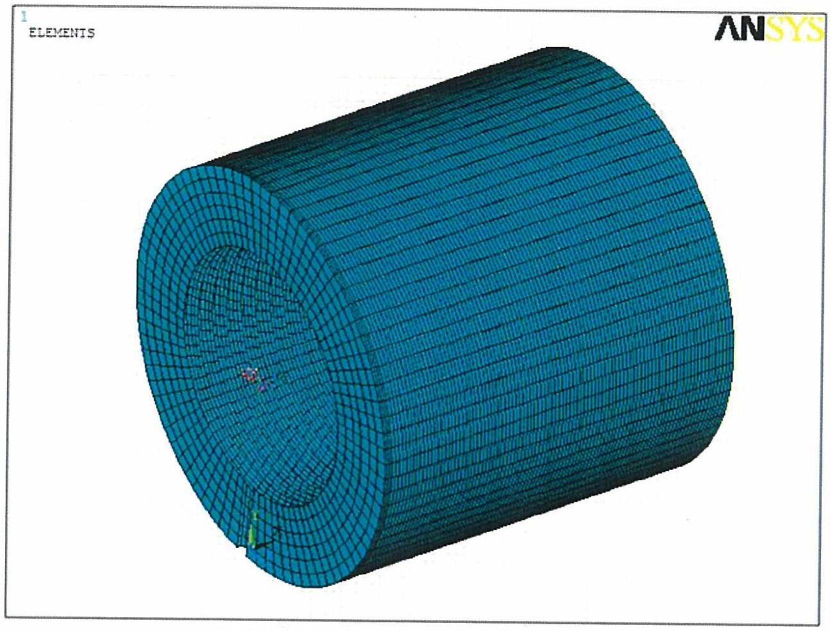

Figure 3-4: Half FEA model of coupling

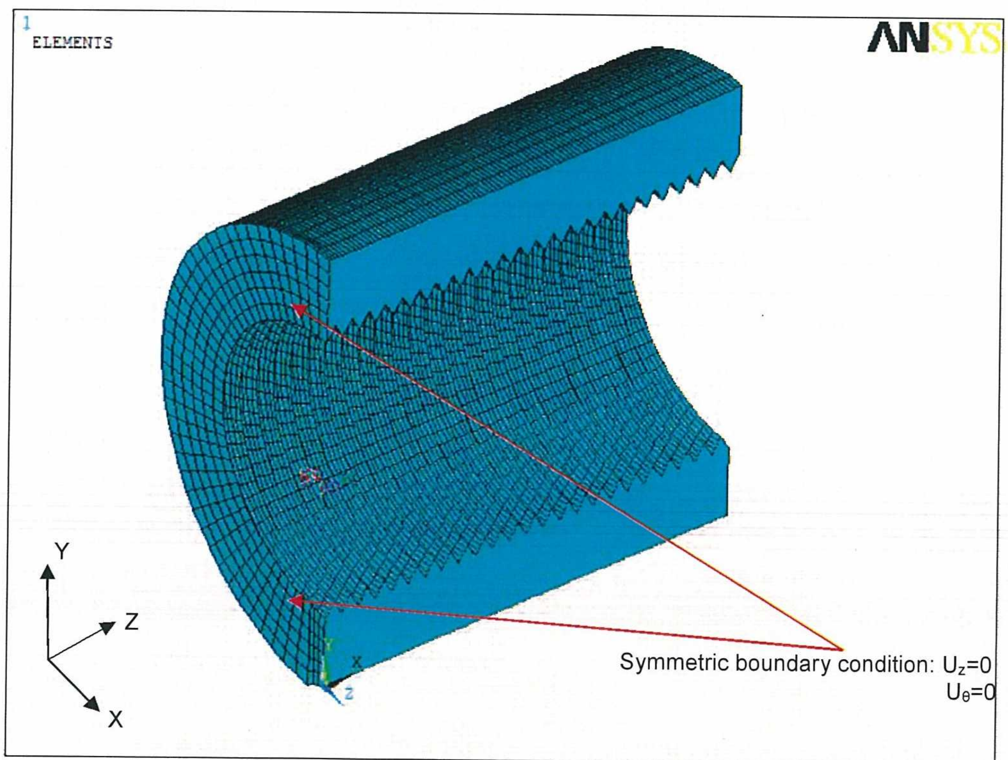

Local coordinate system numbered 11 is cylindrical coordinate system

Figure 3-5: Cross-section of half FEA coupling model

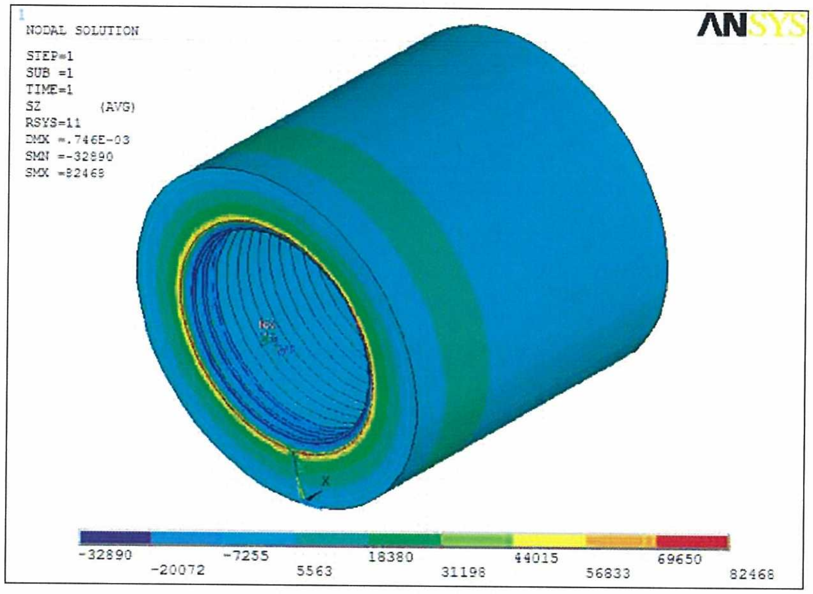

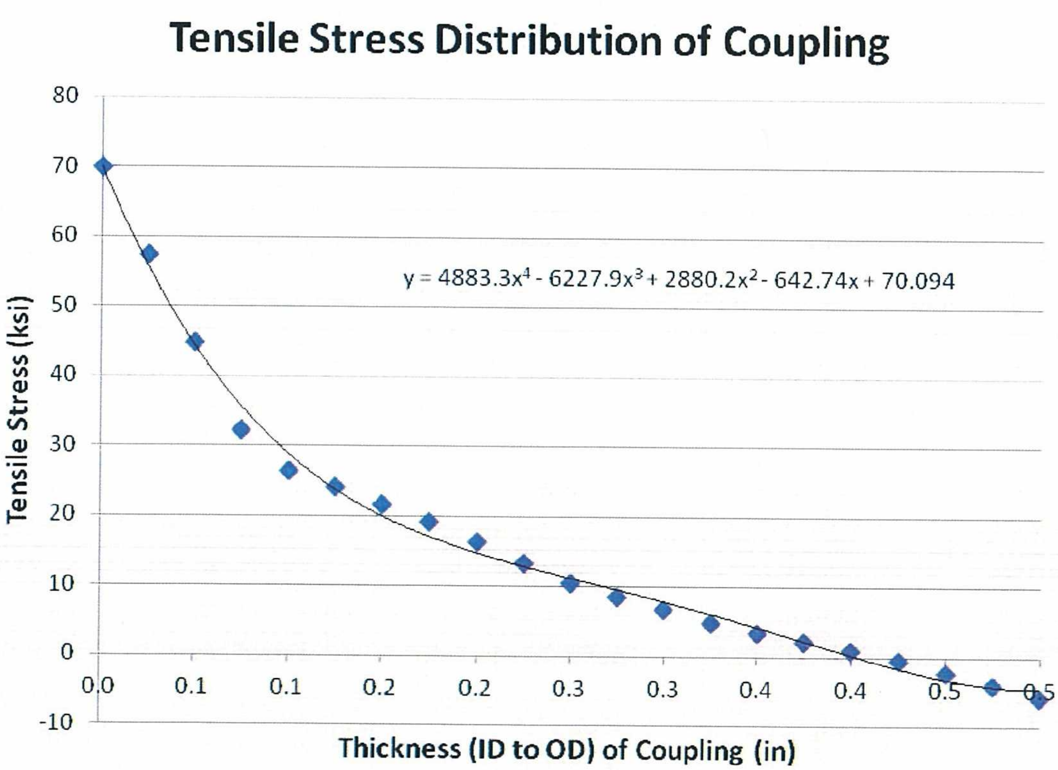

Figure 3-6: Tensile Stress Distribution across Wall Thickness of Coupling (Based on three threads reacting out applied load)

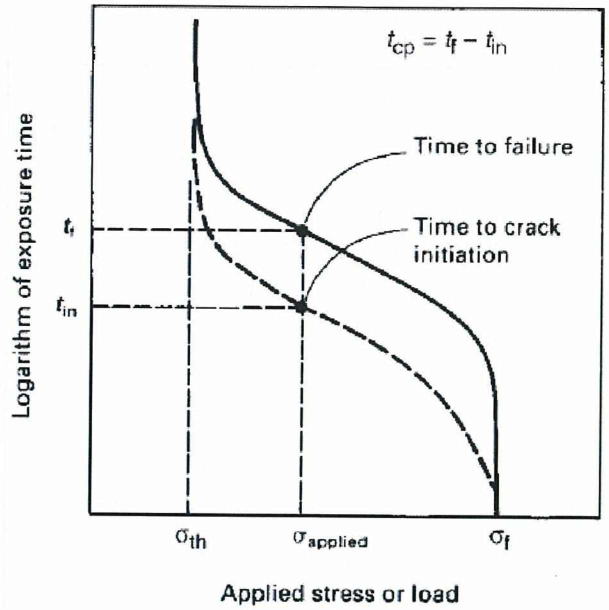

Figure 3-7: Time to Failure vs Applied Stress [8]

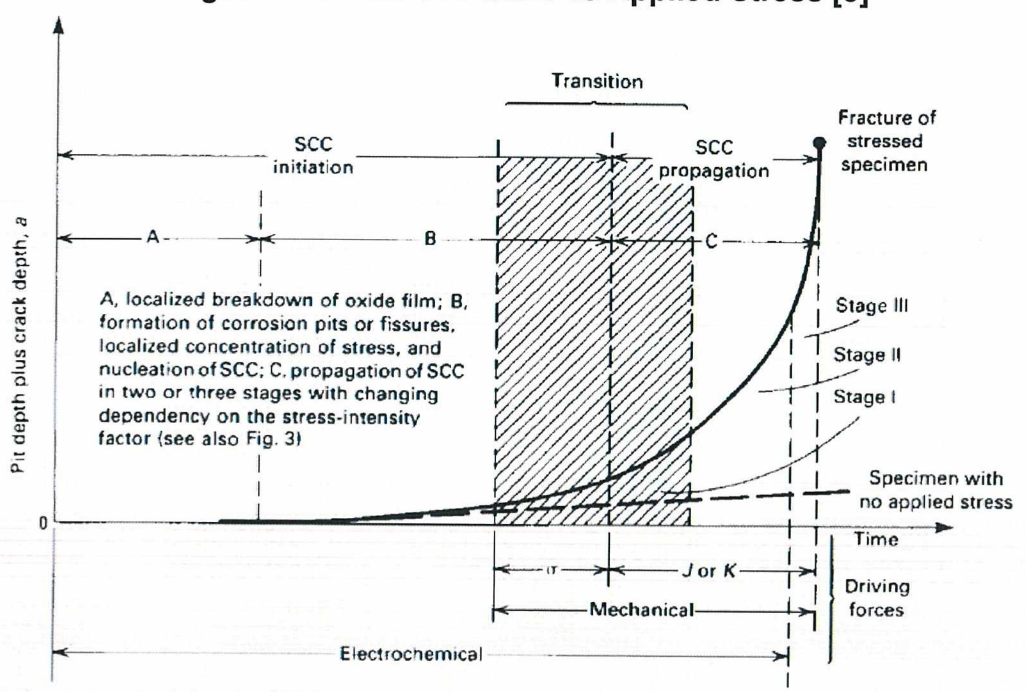

Fig. 2 The relative influences of electrochemical and mechanical factors in the corrosion and SCC damage of a susceptible material. The shaded area represents the transition of driving force from dominance by electrochemical factors to chiefly mechanical factors. Precise separation of initiation and propagation stages is experimentally difficult. Stimulation of cracking by atomic hydrogen may also become involved in this transition region.

Figure 3-8: SCC Process [13]

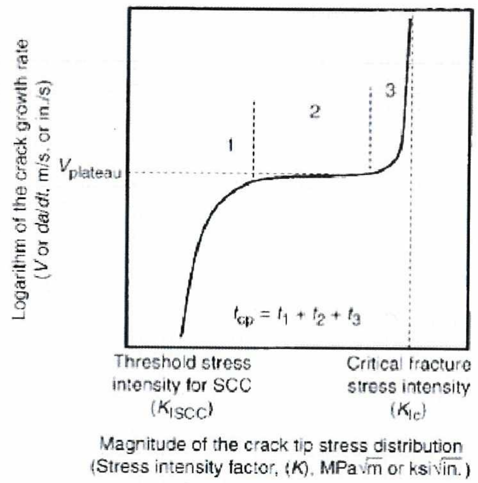

Figure 3-9: Crack Growth Rate (da/dt) versus stress intensity w/Three Stages of Crack Growth [8]

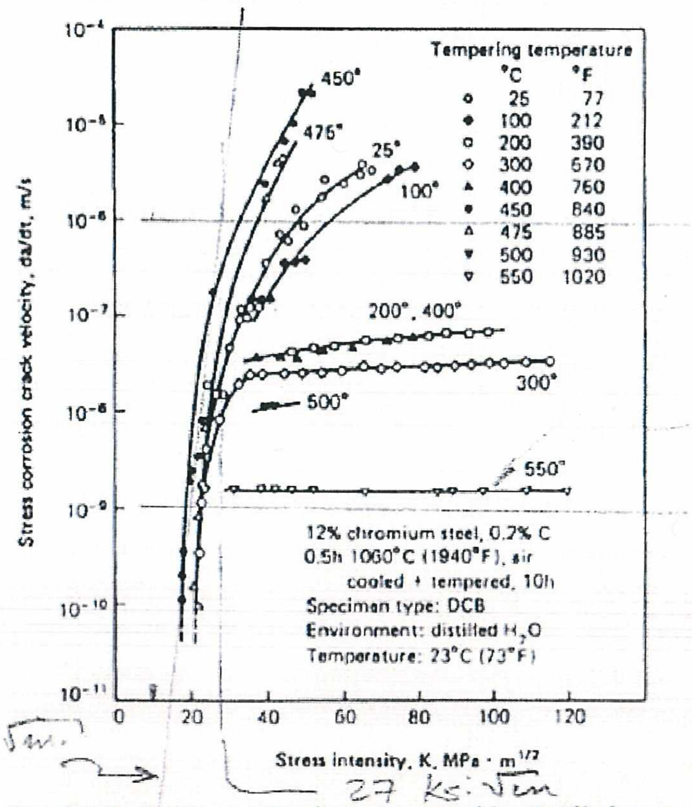

(b) Crack velocity for a 12% chromium steel in distilled water.

Figure 3-10: Effects of Tempering Temperature and Applied Stress-Intensity factor on Velocity of Stress-Corrosion Cracking [7]

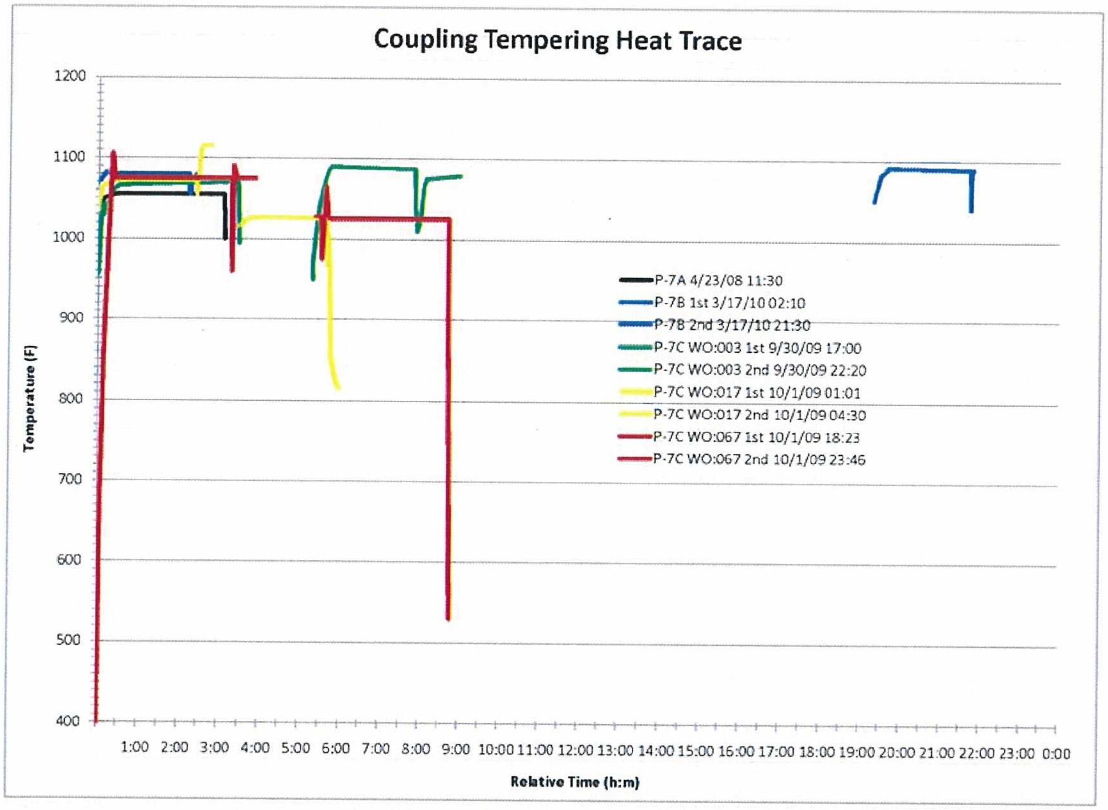

Figure 3-11: SWS Pump Coupling Temperature Trace [3]

$CR_{Kind} := 2.3 \cdot 10^{-4} \frac{in}{hr}$ K independant SCC growth rate

$i := 0..6$ $j := 0..5$

$t_{wall\_meas} := 0.566in$ Min measured wall thickness (include threads)

$TPI := 8$ Couppling threads per Inch

$d_{thread} := 0.625 \cdot \frac{0.866}{TPI} \cdot in$ depth of threads

$t_{wall} := t_{wall\_meas} - d_{thread}$ wall thickness at thread root

$d_{thread} = 0.068\,in$

$t_{wall} = 0.498\,in$

Coupling $CPL_i :=$	Run Time $RT_i :=$	Install Time $IT_i :=$	Depth of crack $d_{crack_i} :=$	Length of crack $L_{crack_i} :=$
"09-P7C-7F"	2414hr	2616hr	t_{wall}	$5 \cdot t_{wall}$
"11-P7C-6F"	14115hr	16224hr	t_{wall}	$5 \cdot t_{wall}$
"11-P7C-7K"	14115hr	16224hr	0.125in	0.86in
"11-P7B-5K"	9073hr	11391hr	0.065in	1.25in
"11-P7B-6K"	9073hr	11391hr	0.132in	0.5in
"11-P7B-7K"	9073hr	11391hr	0.043in	0.5in
"11-P7A-5,6,7"	16259·hr	21024·hr	0.00001in	0.01in

Remaining thickness

$t_{remain} := t_{wall} - \max(d_{crack_2}, d_{crack_3}, d_{crack_4}, d_{crack_5})$

$k := 0..3$

$t_{remain} = 0.366\,in$

$d_{crk_k} := \begin{pmatrix} d_{crack_3} \\ d_{crack_4} \\ d_{crack_5} \\ d_{crack_6} \end{pmatrix}$

$t_{remain_k} := t_{wall} - d_{crk_k}$

Crack Remain Life

$CRL_k := \frac{t_{remain_k}}{CR_{Kind}}$

$CRL = \begin{pmatrix} 78.5 \\ 66.4 \\ 82.5 \\ 90.3 \end{pmatrix} day$ <---B5 <---B6 <---B7 <---A5,6,7

$T_{prop_i} := \frac{d_{crack_i}}{CR_{Kind}}$ Using the K independant growth rate; determine the propagation time

Initiation time is taken to be the elasped time from installation minus the propagation tme.

$T_{init_i} := IT_i - T_{prop_i}$

$\%InitLife_i := \frac{T_{init_i}}{IT_i}$ Percentage of initiation to total life

T_{init} = (day)		T_{prop} = (day)	%InitLife = (%)
19	<-- 09-P7C-7F-->	90	17
586	<-- 11-P7C-6F -->	90	87
653	<-- 11-P7C-7K -->	23	97
463	<-- 11-P7B-5K -->	12	98
451	<-- 11-P7B-6K -->	24	95
467	<-- 11-P7B-7K -->	8	98
876	<-- 11-P7A -->	0	100

Figure 3-12: Coupling Life Estimate for Crack Propagation Across Wall

DESIGN VERIFICATION CHECKLIST

Document No(s)[1]:	F11358-LR-001				Rev.:	0
Review Method:	X	*Design Review*		*Alternate Calculation*		*Test*

	Criteria	DV[2]
1	Were the inputs correctly selected and incorporated into design?	GZ
2	Are assumptions necessary to perform the design activity adequately described and reasonable? Where necessary, are the assumptions identified for subsequent re-verifications when the detailed design activities are completed? If applicable, has an as built verification been performed and reconciled?	GZ
3	Are the appropriate quality and quality assurance requirements specified?	GZ
4	Are the applicable codes, standards and regulatory requirements including issue and addenda properly identified and are their requirements for design met?	N/A
5	Have applicable construction and operating experience been considered, including operation procedures?	N/A
6	Have the design interface requirements been satisfied?	GZ
7	Was an appropriate design method used?	GZ
8	Is the output reasonable compared to inputs?	GZ
9	Are the specified parts, equipment, and processes suitable for the required application?	N/A
10	Are the specified materials compatible with each other and the design environmental conditions to which the material will be exposed?	N/A
11	Have adequate maintenance features and requirements been specified?	N/A
12	Are accessibility and other design provisions adequate for performance of needed maintenance and repair?	N/A
13	Has adequate accessibility been provided to perform the in-service inspection expected to be required during the plant life?	N/A
14	Has the design properly considered radiation exposure to the public and plant personnel?	N/A
15	Are the acceptance criteria incorporated in the design documents sufficient to allow verification that design requirements have been satisfactorily accomplished?	GZ
16	Have adequate pre-operational and subsequent periodic test requirements been appropriately specified?	N/A
17	Are adequate handling, storage, cleaning and shipping requirements specified?	N/A
18	Are adequate identification requirements specified?	N/A
19	Are requirements for record preparation review, approval, retention, etc., adequately specified?	GZ
20	Has an internal design review been performed for applicable design projects? Have comments from the Internal Design Review been appropriately considered/addressed?	N/A

(1) Include any drawings developed from reviewed documents, or include separate checklist sheet for drawings
(2) Design Verifier shall initial indicating review and mark N/A where not applicable

DV Completed By:	*Printed Name* *G. Zysk*	*Signature* [signature] G. Zysk	*Date* *9/28/11*

Page	**1**	**of**	**1**	**Total Pages**	(Include DV Checklist and Comment Resolution sheets in page count)

DOCUMENT SOFTWARE RECORD

(Include Separate Sheet for Each Software Package Utilized)

1	**Computer Software Used** (Code/Version)	ANSYS Version 11.0	
2	**Software Supplier**	ANSYS, Inc.	
3	**Software Update Review**	☒ Error notices; describe: Reviewed error reports for elements used ☐ Other; describe:	
4	**Nuclear Safety Related Software**	☐ NO ☒ YES[1]	1. If YES: Hardware identification # used for execution: *Desktop Serial #: J2WTBM1* Basis for V & V: [15]
5	**Input Listing(s)**	☐ Input listing(s) attached: ☒ Not attached; identify File/Disc ID*: Coupling Pump Bearing & Bending.txt Coupling Pump Bearing.txt Coupling Pump No Bearing.txt *A CD with input listings and output data to be provided on project completion.	
6		☐ Output results attached: ☒ Not attached; identify File/Disc ID*: *A CD with input listings and output data to be provided on project completion.	
7	**Output Identifier(s)***	(see 6 above)	
	*e.g., run date/time; use for reference, as appropriate, within body of calculation		
8	**Comments**		
9	**Keywords****	SOLID45, Static	
	**For use in describing software features used in this calculation; use common terms based on software user manual.		
10	**Project Manager Name:**	S. Yim	

If computer software was used on project, complete form with required information.
Update the LPI Computer Software Use List per LPI Procedure 13.1 requirements.

DOCUMENT INSTRUMENT RECORD				
Instrument Used		Instrument Description	Serial No.	Calibration Due Date
1	☒	Tensile Testing Machine (120 kips)	Baldwin 37205	4/7/12
2	☒	Extensometer (1 in)	2620-824/1033	4/7/12
3	☒	Charpy Impact Tester	Satec Model SI-1K/1306	6/17/12
4	☒	Hardness Tester	Wilson 5YR/58	4/7/12
5	☒	Thermocouple	Omega 650 J/8320	7/12/12
6	☒	Caliper	Fowler 6"/7082002	6/21/12
7	☒	Magnetic Yoke	Magnaflux Y-6/43530	*Per use calibration*
8	☐			
9	☐			
10	☐			
11	☒	SEM/Oxford EDS	17218-118-01	*Per use calibration*
12	☐			
13	☐			
14	☐			
	Project Manager Name:	S. Yim		
For instrument(s) used on the project, identify instrument and include the instrument calibration due date. Update the LPI *Instrument Use List* per LPI Procedure 13.1 requirements.				